POPULATION CONNECTIVITY OF *LOPHELIA PERTUSA* (=*DESMOPHYLLUM PERTUSUM*) IN THE NORTH ATLANTIC OCEAN: PRESENT-DAY CONNECTIONS AND FUTURE PREDICTIONS

By

Graeme Thomas Wiggin Guy

Submitted in partial fulfilment of the requirements

for the degree of Master of Science

at

Dalhousie University

Halifax, Nova Scotia

March 2024

To my Mum, Sue, who continues to motivate me every day.

TABLE OF CONTENTS

LIST OF TABLES

LIST OF FIGURES

ABSTRACT

Population connectivity refers to the exchange of individuals between spatially distinct populations and is an important process governing population dynamics. In species with a larval stage, the combination of processes including reproduction output, timing of spawning, larval development, larval behaviour, settling potential and recruitment rates influence connectivity dynamics. The main objectives of this thesis are 1) to identify spatial and temporal larval connectivity dynamics for *L. pertusa,* an ecologically important species of deep-water coral, and 2) predict changes to the connectivity dynamics with anticipated loss of habitat due to climate change. I use biophysical modelling and graph theory to simulate larval dispersal for *L. pertusa* populations over its known range in the Northwest Atlantic Ocean, identify patterns of potential connectivity and quantify which populations are integral to facilitating these connections. I determine that the timing of spawning has limited influence on the strongest connections observed, but that larval development time and larval behaviour can significantly affect the strength of potential connections. Populations in the north of the domain near Nova Scotia show high local retention rates and strong equatorward connections, following the dominant current directions. Populations in the Gulf of Mexico (GOM) also show high levels of local retention and potential migration to the Southeast United States (SEUS), from Florida to Cape Hatteras. Using a cluster analysis on potential connections, I identify 3 dominant subregions of the domain, the GOM, the SEUS, and the Northern Domain from New England to Nova Scotia, which show alignment with available genetic data. Simulating habitat loss due to climate change shows that existing populations in the GOM and SEUS are likely at higher risk of connectivity disruptions that those in the Northern Domain, with more habitat loss and higher isolation of those that remain. There also appears to be a low probability of larval connection to new areas of suitable habitat anticipated to be available due to climate change. This thesis provides new insights into the connectivity dynamics of an essential deep-sea species and shifts it may experience in a changing environment and contributes to the limited repository of deep-sea connectivity research.

LIST OF ABBREVIATIONS USED

BC = Betweenness Centrality

BNAM = Bedford Institute of Oceanography North Atlantic Model

CCGS = Canadian Coast Guard Ship

DFO = Department of Fisheries and Oceans Canada

EEZ = Exclusive Economic Zone

GOM = Gulf of Mexico

HS = Habitat Suitability

ID = In-degree

LCCA = Lophelia Coral Conservation Area

LR = Local retention

MPA = Marine Protected Area

NAO = North Atlantic Ocean

NE = Northeast

NOAA = National Oceans and Atmospheric Administration

NW = Northwest

OD = Out-degree

PLD = Pelagic Larval Duration

PR = Google Page Rank

RCP = Representative Concentration Pathway

ROV = Remotely Operated Vehicle

SEUS = Southeastern United States

SR = Self-recruitment

SSP = Shared Socioeconomic Pathway

ACKNOWLEDGEMENTS

First and foremost, my deepest gratitude goes to Dr. Anna Metaxas, my supervisor, for her mentorship and the freedom she granted throughout this project. Her commitment to both research support and support in personal matters has been instrumental in bringing this thesis to fruition.

Thank you to my committee members, Drs. Martha Nizinski, Zeliang Wang, and Craig Brown. Martha and Zeliang, for their valuable data contributions, insightful suggestions, and collaborative efforts on manuscripts which have greatly enriched this research journey. Craig Brown, for his wise counsel and suggestions which strengthened this work. I also want to acknowledge and thank Dr. Shuangqiang Wang, who guided me through the intricacies of biophysical modelling during the early stages and provided valuable troubleshooting expertise.

Financial support for this research was generously provided by the National Sciences and Engineering Research Council of Canada (NSERC) Discovery Grant to Dr. Anna Metaxas, along with the NSERC Masters Scholarship (CGS-M). Thank you to the Fisheries and Oceans Canada Oceans Management Contribution Program – "Effective Benthic Habitat Mapping and Monitoring of Marine Protected Areas in Atlantic Canada" for providing financial support. Gratitude also goes to Dalhousie University for their travel grant support.

Thank you to the entire Metaxas lab, past and present. Arieanna Balbar, Sarah De Mendonça, Kylee Lightbody, Matt Mar, Monika Neufeld, Maria Rakka, Conrad Pratt, Alexis Savard-Drouin, and Aaron Ulrick - your camaraderie, idea-sharing, and insightful

feedback on my work were indispensable at all stages of this journey. Many thanks to the Dalhousie Oceanography Student Association (DOSA) for fostering a sense of community and introducing me to many life-long friends.

To my family, whose unwavering support has been instrumental in completing this thesis. Dad, Brian, for instilling a love for science and curiosity in my brother and me as kids. Mum, Sue, for her unlimited support, motivation, and understanding across all aspects of my life. And to my little brother, Thomas, for completing his MSc thesis before me, providing the gentle nudge to strive a little harder.

Finally, to my wonderful partner, Mallory, whose unwavering support, and understanding have been my anchor through the highs and lows. Her constant motivation pushes me to be better every day.

CHAPTER 1

INTRODUCTION

1.1 Background

Population connectivity is defined as the exchange of adults, juveniles, larvae, and genetic information between spatially distinct populations and contributes to a populations overall health and survival (Cowen and Sponaugle 2009). Population connectivity plays a fundamental role in local and metapopulation dynamics by influencing a species spatial structure, genetic diversity and recolonization potential (Cowen et al. 2007; Cowen and Sponaugle 2009). For species with a sedentary adult and a planktonic larval stage, population connectivity is a product of the effects of adult reproduction, larval development and transport, settlement, recruitment into a population, and ultimately survival into a reproductive adult (Pineda et al. 2007). As a result, connectivity dynamics are species and trait specific, and understanding the spatial and temporal scales over which connectivity occurs depends on accurate parameterization of life-history traits (Cowen et al. 2006, 2007).

Numerous techniques exist for estimating connectivity in marine systems, including biophysical modelling, seascape genomics, and tagging, each method with advantages and limitations (Bryan-Brown et al. 2017). Biophysical models, in particular, combine hydrodynamic models with estimated or measured biological variables and allow for the

simulation of larval dispersal on various spatial and temporal scales (Simons et al. 2013). To date, the overwhelming majority of connectivity research has focused on shallow water coral-reefs (Bryan-Brown et al. 2017). For deep-sea species, direct measurements of connectivity are exceedingly rare and difficult to obtain (Gary et al. 2020), and biophysical modelling provides an essential tool. Large knowledge gaps exists for life-history traits in most deep-sea species and biological parameters are not well defined (Hilário et al. 2015). However, biophysical models employing a likely range of parameters can still be useful to explore different scenarios of potential connectivity (Gary et al. 2020).

As with all ocean regions, the deep sea is being affected by climate change (Sweetman et al. 2017). Warming temperatures, deoxygenation, changes to carbon fluxes and acidification are contributing to the degradation of habitat for numerous deep-sea species (Sweetman et al. 2017). Many species have low thermal tolerance to temperatures above their physiological limits and thus low acclimation potential, and adapting to the degradation of habitat will require species to explore new ranges more suitable to their environmental niches (Gunderson and Stillman 2015; Pinsky et al. 2020). In addition, changing ocean conditions will also likely affect life-history stages such as reproduction, larval development, and behaviour (Strömberg and Larsson 2017), having direct consequences for population connectivity.

1.2 Objectives

The overall objective this thesis is to uncover connectivity dynamics for a deep-sea species, and how these dynamics could shift in a changing climate. Specifically, I focus

on the ecologically important deep-sea coral, *L. pertusa,* across its known range in the Northwest Atlantic, from the Gulf of Mexico to the Laurentian Channel. To achieve this, I simulate larval dispersal under present-day oceanographic conditions, quantify dispersal pathways and evaluate how these pathways may change in a changing ocean. This thesis is arranged into 4 chapters, including this Introduction (**Chapter 1**). In **Chapter 2,** I use biophysical modelling and graph theory to model larval dispersal and to infer spatial and temporal connectivity dynamics between present day populations of *L. pertusa*. In **Chapter 3,** I use predictions of habitat degradation due to climate change for the NW Atlantic Ocean to infer how the connectivity dynamics identified in **Chapter 2** may change with the loss of suitable habitat for *L. pertusa*. Then, I evaluate the potential for *L. pertusa* to expand its range in the NW Atlantic by assessing potential connections to areas which may act as climate change refugia. Lastly, in **Chapter 4**, I summarize the main findings of this thesis and how they contribute to the limited body of research on deep-sea connectivity. This work is significant because it reveals fundamental potential connectivity dynamics for an essential deep-water coral over a large portion of its range in the North Atlantic Ocean.

Chapter 2

Stable connections in the deep sea: Temporally consistent larval pathways for the deep-sea coral, *Lophelia pertusa (=Desmophyllum pertusum)* in the Northwest Atlantic Ocean.

2.1 Abstract

Population connectivity facilitates genetic exchange and increases resilience of populations promoting long-term stability. For sessile benthic invertebrates, larval dispersal provides the main mechanism to achieving population connectivity. Biophysical modelling of larval dispersal can quantify dispersal pathways, and when combined with graph theory analysis can elucidate potential connections between populations and evaluate their potential importance to the stability of the entire network. We use these tools to examine the dispersal pathways of the deep-water coral *Lophelia pertusa* (=*Desmophyllum pertusum*) over its North American range in the Northwest Atlantic Ocean. We used a high-resolution ocean circulation model in combination with larval parameters for *L. pertusa*, to project larval dispersal for each season over 14 years from 2005-2018. We then used the strength and number of connections between populations to quantify the importance of each population to the overall connectivity within the network. Larval retention was strongest in the north of the domain and within the Gulf of Mexico. The two dominant transport pathways occurred following the Gulf Stream from Florida north towards the eastern United States and following the Labrador Current travelling southwestwards from the Canadian EEZ with little exchange between northern and southern domains. Our graph theoretic analysis suggested that the populations of *L. pertusa* in Norfolk Canyon are primarily responsible for exchange between northern and southern populations; however, no northward connections were projected. The results of a cluster analysis based on population connectivity agree well with previous patterns based on estimates of genetic connectivity in the area. The observed dominant connection pathways remained consistent throughout spawning seasons, years, and for biological parameters, emphasizing the utility of connectivity analyses for deep-water species with unresolved life-history traits.

2.2 Introduction

Larval dispersal and subsequent settlement facilitate connections between geographically distant populations, enabling genetic exchange and the replenishment of damaged or depleted communities (Berumen et al. 2012; Cecino and Treml 2021). Understanding these specific connections is fundamental to understanding the survival, recovery, and adaptive capabilities of marine organisms.

In marine environments, larval dispersal is affected by numerous biotic and abiotic factors, such as spawning seasonality and location, pelagic larval duration (PLD), ocean current dynamics, and larval buoyancy and behaviour (Hilário et al. 2015; Treml et al. 2015; Strömberg and Larsson 2017; Cecino and Treml 2021; Matos et al. 2023). Due to fine-scale spatial and temporal variability in some current regimes, the timing and location of spawning can greatly affect larval transport (Roughan et al. 2011). PLD, or the amount of time larvae spend in the water column, has been identified as the factor most greatly affecting the magnitude of dispersal distance, with longer PLD generally facilitating greater dispersal (Treml et al. 2015). PLD combines two periods, pre-competency during which larvae are still not developed enough to settle onto the benthos, and competency during which larvae are presumed to settle on suitable substrates (Larsson et al. 2014). Larval traits which affect the vertical position in the water column, such as buoyancy and swimming behaviour, can also greatly affect dispersal capabilities, because of depth-related differences in current velocities (Fox et al. 2016). These factors, along with those regulating larval settlement, dictate the potential connectivity between populations. Rates of larval development determine larval pre-competency period, or the

time it takes larvae to develop into competent settlers, which is in turn affected by factors such as temperature (Strömberg and Larsson 2017). Faster development rates may result in increased local settlement in natal regions or in populations separated by small distances (Treml et al. 2015).

By integrating biological processes, such as spawning season, larval development, mortality, and behavior, with physical factors such as ocean currents, temperature, and salinity, biophysical models can predict larval dispersal patterns (Connolly and Baird 2010; Cardona et al. 2016; Assis et al. 2021). Using these predictions, graph theory can be used to create network models that represent real world metapopulations (networks of interconnected local populations). Habitat patches are represented as vertices (nodes) in the network and the dispersal linkages (connections) as the edges within the network (Urban et al. 2009). Spatial and temporal patterns of connectivity can be quantified and the most important nodes within the network identified through various node and network level connectivity metrics (Cecino and Treml 2021).

In the deep ocean, structure-forming deep-water corals serve as intricate biological hotspots, providing habitat for numerous marine species. Their frameworks provide shelter, breeding sites, and feeding grounds for many organisms, including fishes and invertebrates, in an environment where structure can be sparse (Baillon et al. 2012; De Clippele et al. 2015; Auscavitch et al. 2020). *Lophelia pertusa* (= *Desmophyllum pertusum*)[1], is a cosmopolitan structure forming deep-water coral species found at

[1] A taxonomic change from *L. pertusa* to *D. pertusum* has been proposed (Addamo et al. 2016) and now accepted in the World Register of Marine Species (WoRMS) database (Hoeksema and Cairns 2023). However, we agree with Dr. Steve Cairns (WoRMS database editor) to exercise caution in changing nomenclature until more research is done and elect to use the older nomenclature herein.

temperatures ranging from 4 to14°C, depths from 200 meters to over 1,000 meters, and areas of moderate current velocities (Pires et al. 2014; Brooke and Ross 2014; Ross et al. 2015; Kenchington et al. 2017; Sundahl et al. 2020; Tong et al. 2022). *Lophelia pertusa* is particularly abundant in the North Atlantic Ocean, where it can form extensive reef structures (Brooke and Schroeder 2007; Ross and Nizinski 2007; Wheeler et al. 2007; Buhl-Mortensen et al. 2017). Periodic broadcast spawning occurs during the winter months in the NE Atlantic with slight variation between geographic locations (Waller and Tyler 2005; Larsson et al. 2014). The underlying mechanisms for differences in spawning times between geographic locations is unclear but could be due to external environmental variables, such as temperature and food supply, which regulate the timing of planular release (Waller and Tyler 2005; Harrison 2011; Mercier et al. 2011; Baillon et al. 2014). Larvae of *L. pertusa* are planktotrophic and free-swimming, and their rate of development has a significant, positive relationship with temperature (Strömberg and Larsson 2017). Larvae exhibit upwards vertical migration during development and downwards bottom-probing behaviour once competent to settle; the length of the larval pre-competency period is at least 3 weeks at 7-8°C but can be as short as 2 weeks in warmer water (Strömberg and Larsson 2017). Differences in temperature and current velocity among depths and geographic locations affect spawning times, larval development, and pre-competency period, thus having a significant impact on population connectivity (Strömberg and Larsson 2017).

In this study, we examine the effect of spawning season, length of pre-competency period and swimming velocity on larval dispersal and connectivity of *L. pertusa* in the NW Atlantic. We use a high-resolution biophysical model, which incorporates known

larval biological parameters (larval duration and behaviour), to release larvae three times per season from known populations of *L. pertusa* ranging from the Gulf of Mexico to Nova Scotia, Canada, from 2005-2018. Using graph theory to examine the dispersal tracks, we identify which populations of *L. pertusa* are the most important for maintaining connectivity within the NW Atlantic, which areas are most isolated, where the strongest connections occur, and whether these connectivity patterns vary with season, length of pre-competency period and/or swimming velocity. Such knowledge is critical for marine conservation and management, particularly when establishing marine protected areas or assessing the potential impacts of human activities, like fishing and coastal development. Additionally, this study highlights how biophysical models can be used to estimate connectivity for deep-sea species, including those whose life-history traits are not well understood.

2.3 Methods

2.3.1 Data Collection

We assembled presence records from several sources including video surveys by Remotely Operated Vehicle (ROV) on the NOAA ship *Okeanos Explorer* during the research cruise EX1905 (2019), ROV video and trawl surveys performed by Fisheries and Oceans, Canada (DFO) on the *CCGS Hudson* (2003-2018), NOAA's Deep-Sea Coral Data Portal (1968-2019), and Martha Nizinski (NOAA, ROV video and towed-camera imagery 2012-2017). These data represent locations from continental shelf and slope habitats in the Gulf of Mexico, to off the east coast of Florida, northwards to off the

Scotian Shelf, from 52 to 1488 m depth (Figure 2.1). A detailed list of each research cruise and data source is provided in Supplementary Table A2.1. These data were filtered to remove duplicate observations, observations where corals were identified as 'dead', and observations with location accuracy being 'unknown' or '>1000m'. The resulting 3780, highly clustered, observations of individual colonies of *L. pertusa*, were aggregated over a 0.1ºx0.1º spatial grid, with *L. pertusa* occurring in 105 grid cells in the domain.

2.3.2 Study Domain

The domain was restricted to the Northwest Atlantic, spanning from within the Gulf of Mexico in the southwest to the Laurentian Channel at the northeast boundary (Figure 2.1). The region is dominated by two energetic western boundary currents in the North Atlantic Ocean - the Gulf Stream and Labrador Current, and an on-shelf current – the Nova Scotia Current. The warm northward travelling Gulf Stream exits the Gulf of Mexico and travels north along the shelf break before separating from the continental shelf near Cape Hatteras, North Carolina, and then advances eastwards towards the Grand Banks, forming complex meandering eddies (Rossby et al. 1985; Rossby and Benway 2000; Bisagni et al. 2017; Seidov et al. 2019). The cold Labrador Current originates in high latitudes in the north and flows equatorward along the shelf break. A confluence zone between the Gulf Stream and the Labrador Current forms in the off-shelf region (Han et al. 2010) (Figure 2.1). The Nova Scotia Current originates in the Gulf of St. Lawrence and enters the Scotian Shelf through the Cabot Strait, flowing on the Scotia Shelf into the Gulf of Maine, where it forms a counterclockwise mean circulation (Townsend et al. 2006). The upper 800-1000 m in the Gulf of Mexico are dominated by the anticyclonic Loop Current (LC) which flows clockwise around the basin from the

Yucatan Channel to the Florida Straights, with anticyclonic mean near-bottom circulation (DeHaan and Sturges 2005).

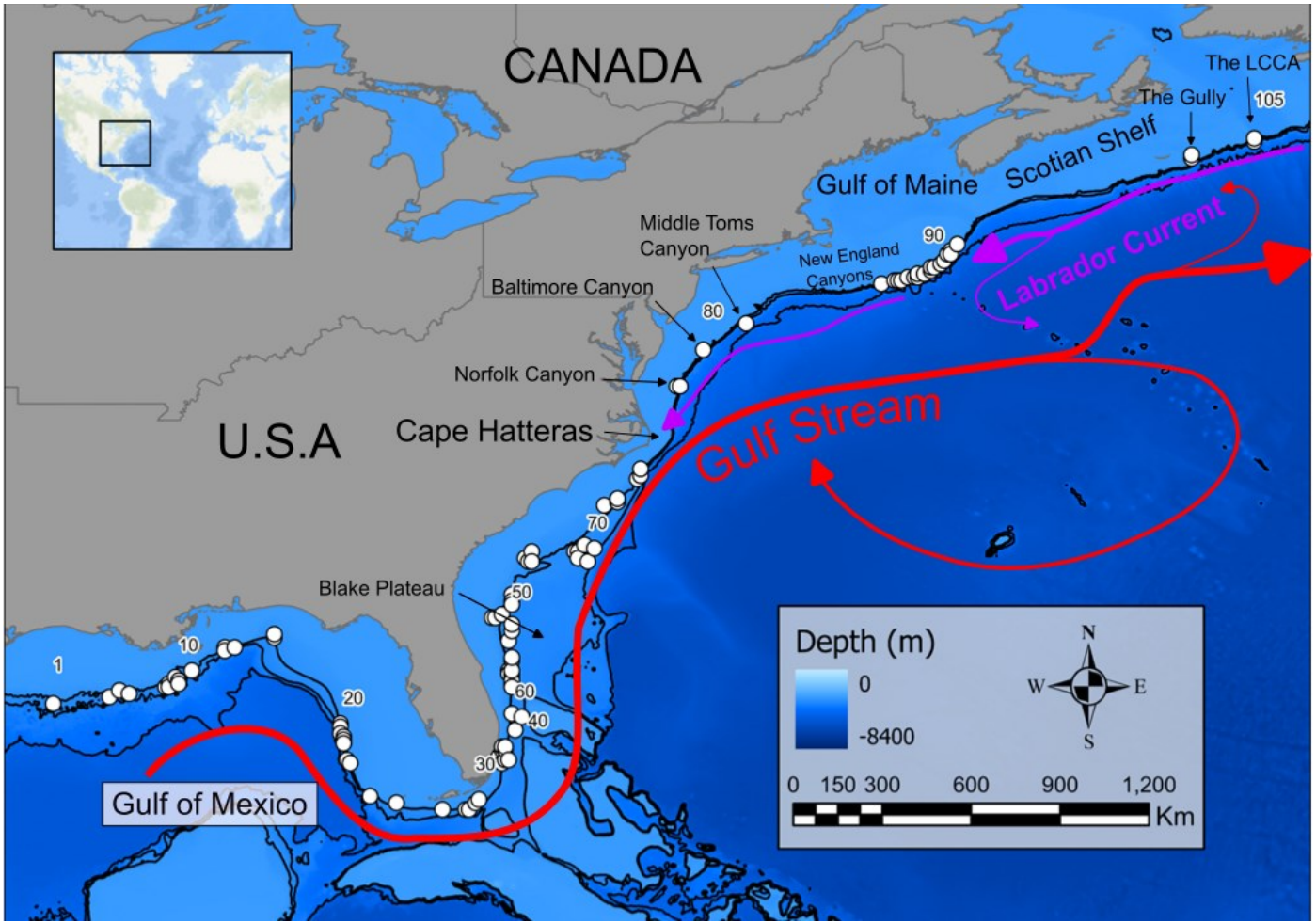

Figure 2.1 – Map of the domain included in the study. White points show locations of particle release, numbered from west to east. Distinctive local geography and dominant currents are shown. The inset map shows the location of the domain on a global map.

2.3.3 Dispersal Simulation

We extracted 3-D hydrodynamic currents of the North Atlantic Ocean from the eddy resolving BNAM (Bedford Institute of Oceanography North Atlantic Model), which is based on version 2.3 of NEMO (Nucleus for European Modelling of the Ocean), a framework for ocean modelling (https://www.nemo-ocean.eu/.). BNAM covers the entire North Atlantic Ocean, with grid sizes of 2.7 km (zonal direction) and 2.1 km (meridional direction) in the northernmost part of the domain and increases to a maximum of 9.17 km at the southern boundary of the domain. There are 50 vertical layers, varying in thickness from 1 m at the surface to 450 m at the seabed. BNAM currents have been ground-truthed and agree well with the surface currents derived from surface drifter data and with the bottom currents from current meter data (Wang et al. 2018). Monthly-mean current data for 2005-2018 were extracted from BNAM for the spatial domain bounded by the 60º-17ºN parallels and 48º-95ºW meridians.

We ran 3-D particle tracking simulations using OceanParcels v2.4.0 Lagrangian Framework (Delandmeter and van Sebille 2019) on the ocean circulation data extracted from BNAM. Simulated particles were advected in the Parcels framework using the fourth order Runge-Kutta method. Each 0.1ºx0.1º grid cell containing *L. pertusa* was seeded with particles at an equal spacing of 0.003º, which equalled 1156 particles per cell, for a total of 121,380 particles over the entire domain. To determine this optimal spacing for the particles, i.e., one which produced consistent results with the minimum computational load, we ran trials for different particle spacing over a subset of the temporal and spatial range of the domain. Specifically, we ran particle tracking simulations for particle spacings of 0.01, 0.005, 0.003, and 0.001 for January, March,

May, and July 2005, 2006, and 2007, from Florida to Nova Scotia (i.e. excluding the Gulf of Mexico). We compared the resulting particle density distributions using the fraction of unexplained variance (FUV), calculated as

$$FUV = 1\text{-}r^2 \text{ (Simons et al. 2013),}$$

where r is the linear correlation coefficient between two different particle density distributions. Very low FUV's (<0.05) were obtained between particle spacings of 0.003 and 0.001, showing that the outputs of the model were highly correlated. We chose a spacing of 0.003 for subsequent model runs, as trials at 0.001 increased computational load significantly. We ran the model in forecast mode using monthly mean currents, and tracked particles released on the 1st day of each month from January 2005 to December 2018 for 60 days at time steps of 10 minutes, to ensure particles did not cross an entire grid cell in a single time step (Wang et al. 2019). We condensed the monthly model outputs into seasonal outputs by adding January, February, March (Winter); April, May, June (Spring); July, August, September (Summer); and October, November, December (Autumn) together to form 4 seasons per year, which were then averaged over 2005-2018.

We included random horizontal particle movement in the model to simulate ocean processes not resolved by the model, using a horizontal diffusivity constant, K_h (cm^2s^{-1}), based on Okubo's (1971) 4/3 power law relationship:

$$K_h = 0.0103l^{4/3}$$

l (cm) is the scale of diffusion and depends on the spatial resolution of the ocean model (BNAM), which varies with latitude over the study domain (Wang et al. 2022).

Therefore, K_h values were calculated for each grid cell, and varied from 25.8584 m^2s^{-1}, in the north, to 91.8797 m^2s^{-1}, in the south.

We included several biological parameters in the model, which were either fixed based on existing knowledge such as from laboratory experiments (e.g., planktonic larval duration) or ranging to explore different scenarios (e.g., spawning season, larval swimming velocity) (Table 2.1). Vertical swimming velocity (larval behaviour) was directed towards the surface during the pre-competency period and altered to bottom-probing behaviour once larvae reached competency. For each of 20- and 30-day pre-competency period, we ran dispersal trials for each of two different patterns of vertical velocity: (1) velocity increased linearly from 0 mms^{-1} on day 0 to a maximum of 0.88 mms^{-1} at the end of the PLD (Strömberg and Larsson 2017); and (2) from day 0 of the model run, we randomly selected velocity values each day from a velocity distribution of 0.72 ± 0.18 mm s^{-1}. Due to the time required for larvae to develop cilia (fully ciliated at ~ 2 weeks post-fertilization - Larsson et al. 2014) and stronger swimming capabilities, we consider the scenario (1) of larval behaviour the most representative of real-life dispersal and report results in terms of this trial run. Reporting on each run individually is redundant as there are strong similarities between trials; therefore, we have identified and discussed differences between trials where they exist.

Table 2.1 Parameters included in dispersal simulation model runs for *Lophelia pertusa*.

Parameter	Value	Rationale	Source
Spawning season	Winter (Jan-Mar) Spring (April-June) Summer (July-Sept) Autumn (Oct-Dec)	Unknown spawning season in NW Atlantic	Stromberg, Larsson et al. 2017
Larval releases	t=0, t=30 and t=60 days each season	Studies show multiple gamete releases over spawning period	Brooke & Jamegren, 2013 Larsson et al. 2014
Pelagic Larval Duration (PLD)	60 days	~57 days in the laboratory (NE Atlantic colonies)	Stromberg & Larsson, 2017 Larson et al. 2014
Pre-competency period	20 days, 30 days	Larvae only competent to settle after 20 and 30 days	Stromberg & Larsson, 2017 Larson et al. 2014
Vertical swimming velocity (Larval behaviour 1)	Linear increase from 0 to 0.88 mms^{-1} over 60 days	Max swimming velocity measured in laboratory	Stromberg & Larsson, 2017
Vertical swimming velocity (Larval behaviour 2)	0.72 ± 0.18 mms^{-1}	Mean velocity measured in laboratory from 36-day old larvae	Stromberg & Larsson, 2017 Larson et al. 2014
Horizontal diffusivity constant - k_h	25.9 m^2s^{-1} - 91.9 m^2s^{-1}	Scale depends on BNAM resolution, which varies with latitude	Okubo 1971 Wang et al. 2022
Release depth	Seabed	Natural release point of larvae	

2.3.4 Network Analysis

To estimate connectivity from the particle trajectories, we calculated probability matrices, which show the probability that a particle will travel from source cell *j* to receiving cell *i*. Rows in the matrix represent source cells and columns represent receiving cells, and the value of each cell is the probability that a connection will occur. We defined connection probability as the number of particles which travel from source cell *j* to receiving cell *i*, divided by the number of particles released at source cell *j*. For each season, we calculated mean connection probability over the period 2005-2018 using all matrices over the 14-year period.

We applied graph theory to quantify relationships between source and receiving cells, to calculate connectivity metrics and to detect communities of *L. pertusa* within the network. In a graph, cells in the probability matrices are represented as nodes and connections between nodes as directed edges, which are edges that can only occur in a single direction. We selected 2 indices of self persistence, local retention (LR) and self-recruitment (SR), and 4 measures of centrality, in-degree (ID), out-degree (OD), betweenness centrality (BC) and Google PageRank (PR), which have been recommended particularly for MPAs (metric details in Table 2.2) (Ospina-Alvarez et al. 2020). Self-persistence refers to the ability of a local population (node) to persist independently of input from other populations within the network (Burgess et al. 2014). Measures of centrality identify the most important nodes within a network by evaluating their connection strength, number of connections, and how frequently they appear on the shortest paths between other nodes.

Table 2.2 Measures of persistence indices and centrality measures used in the network analysis to quantify connectivity. See references for additional information.

Measure	Definition	Calculation	Rationale	Reference
Local retention (LR)	The ratio of the number of locally produced larvae which remain at the site after the dispersal period to the total number of locally produced larvae	LR is equal to the diagonal elements of the probability matrix	LR identifies nodes which retain a large portion of the larvae produced at that node and may indicated a stronger potential to be self-sustaining	Lett et al. 2015
Self-recruitment (SR)	The ratio of the number of locally produced larvae which remain at a site to total number larvae which arrive from all other locations	SR is equal to the diagonal elements of the probability matrix divided by the sum of the corresponding column of the probability matrix	SR identifies nodes where recruitment is largely composed of larvae which originated at that node	Lett et al. 2015
In-degree (ID)	The number of incoming connections (edges) to a node, irrespective of strength	$\sum$ incoming connections (unweighted)	ID identifies nodes which receive larval input from many other nodes, and could result in higher genetic diversity and population resilience	Minor and Urban 2007

Table 2.2 Continued…

Measure	Definition	Calculation	Rationale	Reference
Out-degree (OD)	The number of outgoing connections (edges) from a node, irrespective of strength	∑ outgoing connections (unweighted)	OD identifies nodes which supply larvae to many other nodes and may have a large influence on network wide dynamics	Minor and Urban 2007
Betweenness centrality (BC)	Measure of the number of shortest paths between 2 nodes, which pass through the focal node	*see documentation of the 'igraph' package in Python	BC identifies nodes which may act as stepping-stones between other nodes and facilitate dispersal through the network	Minor and Urban 2007
Google PageRank (PR)	PR uses the number and strength of connections between nodes to estimate the overall importance of the node in a graph. It ranks the nodes based on the local density of in and out connections to other nodes in the network	*see documentation of the 'igraph' package in Python	PR identifies nodes which are critical to maintaining connectivity within the overall network	Kininmonth et al. 2019

Communities were detected using the Leiden algorithm which assigns individual nodes to communities based on the number of connections between those nodes (i.e. communities are groups of nodes which have a high number of connections between them) (Traag et al. 2019). The Leiden algorithm involves 3 phases: (1) assign nodes to communities; (2) refine communities; (3) aggregate the nodes based on the refinement. The algorithm repeats this process until all nodes are optimally assigned. To assess the strength of the community divisions, we used the benefit function, *Q*, a measure of how confidently a graph can be separated into communities. *Q* ranges from 0 for a completely random graph to 1 for a graph with a high number of connections within communities and minimal connections between communities (Leicht and Newman 2008).

For a directed network, *Q* is defined as:

$$Q = \frac{1}{m}\sum_{ij}(A_{ij} - \frac{k_i^{out}k_j^{in}}{m})\partial(\sigma_i, \sigma_j)$$

where A_{ij} is an element of the connectivity matrix (value of 1 if there is an edge from *j* to *i* and 0 otherwise), k_i^{out} and k_j^{in} are the in- and out- degrees of the nodes, *m* is the total number of connections in the network, σ_i denotes the community of node *i* and $\partial(\sigma_i, \sigma_j)$ = 1 if $\sigma_i = \sigma_j$ and 0 otherwise (Supplementary Figure A1) (Leicht and Newman 2008).

2.4 Results

In reporting and discussing the results of this thesis, we employ the term 'population', 'node', and 'cell' interchangeably depending on whether the context is biological, relating

to specific aspects of a graph, or relating to a matrix, respectively. The model predicted many connections and few isolated populations for all 4 seasons, with some seasonal and interannual variability (Figure 2.2; 2.3; Supplementary Figures A2-5). Mean connection probability was highest in summer and lowest in winter for all dispersal simulations. However, this pattern was only significant for the dispersal simulation with larval behaviour 1 and 30-day pre-competency period. For the remainder of the dispersal simulations, there was no significant differences in mean connection probabilities between seasons for model runs with the same pre-competency period and larval behaviour (Table 2.3). Connection probabilities were significantly higher for particles with a 20-day than 30-day pre-competency period for all seasons and both larval behaviours. Although the patterns of connections remained the same, the strength of most connections increased twofold. Similarly, connection probabilities were significantly higher and increased twofold for particles exhibiting larval behaviour 1 than larval behaviour 2 for the same pre-competency period (Figure 2.2A, C; 2.3 A, C; Table 2.3). For all dispersal simulations, the mean number of yearly connections was significantly higher in winter and autumn than in spring. The total possible number of connections was also highest in winter and lowest in spring, except for larval behaviour 1 and a pre-competency period of 20 days, where the number of connections was highest in autumn (Table 2.3

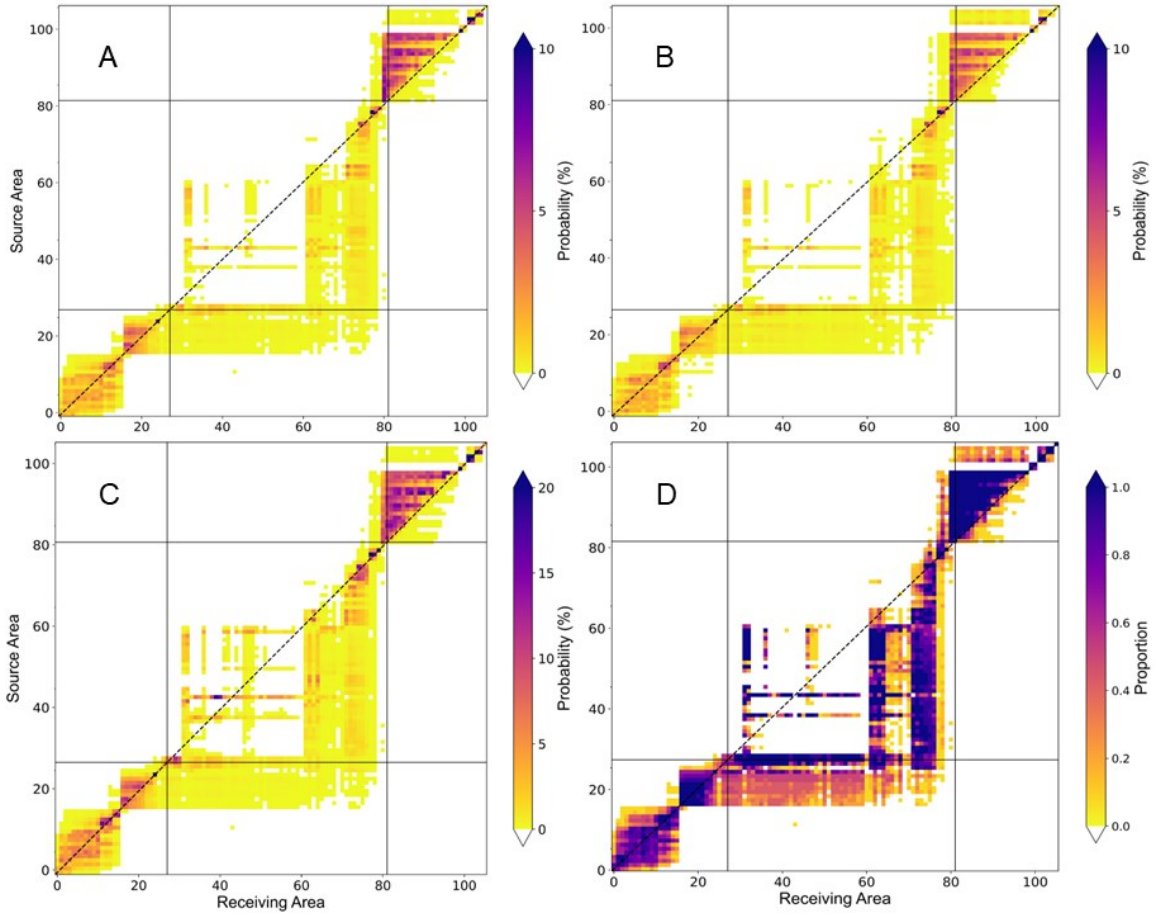

Figure 2.2 – **A/B**- Connection probabilities for particles traveling from source cell i (vertical axis) to receiving cell j (horizontal axis) for summer (**A**), and winter (**B**) averaged over 2005-2018, for particles with a 30-day competency period with larval behaviour 1 (swimming velocity varying across development). The dashed, diagonal line (i=j) shows areas of local retention. **C**- Connection probabilities for summer averaged over 2005-2018 for particles with a 20-day competency period. **D**- Cells show the proportion of years a connection occurs over of the 14-year period of summer 2005-2018. Darker colours indicate connections which occur regularly on a yearly basis. The 4 solid lines (2 vertical and 2 horizontal) represent 12.5º degrees of longitude divisions within the study domain, at -81.5º W and -69º W. Coloured cells below the dashed horizontal line represent transport towards the east, and coloured cells above the dashed horizontal line represent transport towards the west.

Table 2.3 – Summary of connections for each model run. Larval behaviour 1 is a linear increase in vertical velocity from 0 mms^{-1} at day 0 to 0.88 mms^{-1} at day 60, and Larval behaviour 2 is a randomly sampled velocity from a normal velocity distribution of 0.72 ± 0.18 mms^{-1}. Total possible connections are the sums of all unique connections that occurred for that season in 2005-2018. Mean number of connections is the average number of connections that occur per season over the 2005-2018 period, with associated standard deviations (SD). Mean connection probability is the mean probability of all connections in a season, averaged over 2005-2018. Significant differences in number of connections and connection probabilities between seasons and pre-competency periods were identified using the Tukey's Honestly Significant Differenced test (HSD). Matching superscripts indicate no significant difference among values. Number of clusters is the number of clusters identified from the connectivity matrices averaged over 2005-2018 for each season, and their corresponding modularity score, *Q*. *Q* ranges from 0 for an unstructured, random graph to 1 for a graph with numerous connections within communities and no connections between communities.

Season	**Years (20** - 20**)**	**Larval behaviour**	**Pre-competency period (days)**	**Total possible connections**	**Number of connections (m± SD, n=14)**	**Connection probability (m± SD, n=14)**	**Number of clusters**	***Q***
Winter	05-18	1	30	2249	1326.5 ± 109.3 ^{a}	1.09 ± 1.77 ^{e}	6	0.38
Spring	05-18	1	30	2080	1173.5 ± 123.3 ^{b}	1.25 ± 1.96 $^{e, f}$	6	0.39
Summer	05-18	1	30	2232	1220.5 ± 169.3 $^{a, b}$	1.30 ± 2.02 ^{f}	6	0.41
Autumn	05-18	1	30	2190	1321.79 ± 114.9 $^{a, b}$	1.19 ± 1.86 $^{e, f}$	6	0.40
Winter	05-18	1	20	2492	1613.57 ± 101.8 ^{c}	2.47± 4.19 ^{g}	6	0.37
Spring	05-18	1	20	2374	1476.5 ± 121.6 ^{d}	2.75 ± 4.48 ^{g}	6	0.38
Summer	05-18	1	20	2482	1507.36 ± 175.6 $^{c, d}$	2.81 ± 4.55 ^{g}	6	0.39
Autumn	05-18	1	20	2515	1610.43 ± 121.4 ^{c}	2.57 ± 4.21 ^{g}	6	0.36
Winter	05-18	2	30	1779	625.8 ± 123.2 $^{i, k}$	0.49 ± 0.83 ^{o}	5	0.46

Table 2.3 Continued…

Season	Years (20** - 20**)	Larval behaviour	Pre-competency period (days)	Total possible connections	Number of connections (m± SD, n=14)	Connection probability (m± SD, n=14)	Number of clusters	*Q*
Spring	05-18	2	30	1510	489.9 ± 62.6 [j]	0.62 ± 1.13 [o]	6	0.48
Summer	05-18	2	30	1656	501.5 ± 120.5 [i, j]	0.66 ± 1.20 [o]	6	0.53
Autumn	05-18	2	30	1769	665 ± 84.2 [k]	0.6 ± 1.02 [o]	5	0.47
Winter	05-18	2	20	1949	825.2 ± 132.22 [l, m]	1.05 ± 1.78 [p]	4	0.45
Spring	05-18	2	20	1712	683 ± 84.9 [n, o]	1.19 ± 1.99 [p]	6	0.42
Summer	05-18	2	20	1861	715.1 ± 155.5 [m, o]	1.27 ± 2.05 [p]	6	0.50
Autumn	05-18	2	20	1923	862.1 ± 99.2 [l]	1.24 ± 2.01 [p]	5	0.47

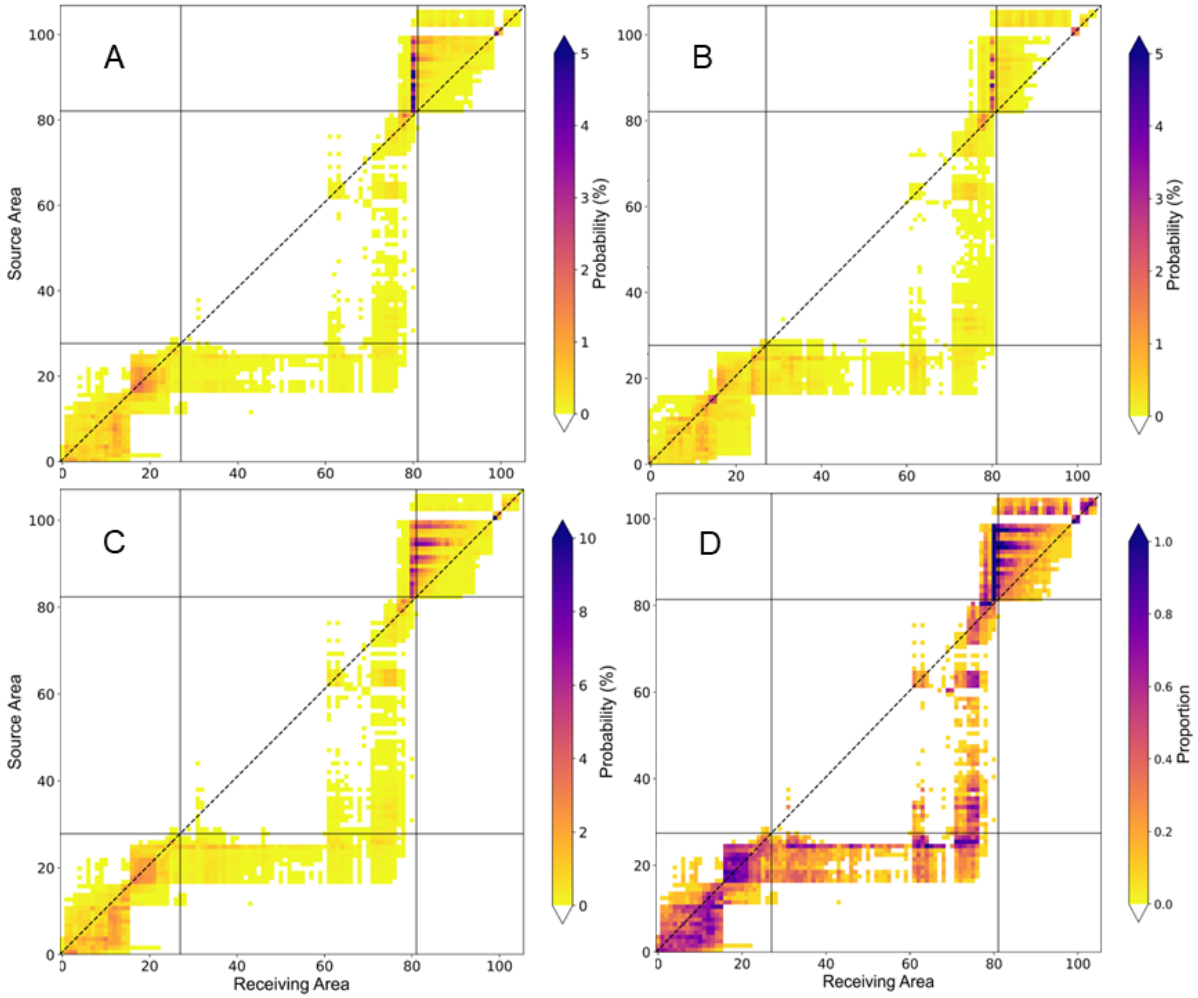

Figure 2.3 - Connection probabilities for particles traveling from source cell i (vertical axis) to receiving cell j (horizontal axis) for summer (**A**), and winter (**B**) averaged over 2005-2018, for particles with a 30-day competency period with larval behaviour 2 (constant velocity over development). The dashed, diagonal line (i=j) shows areas of local retention. **C**- Connection probabilities for summer averaged over 2005-2018 for particles with a 20-day competency period. **D**- Cells show the proportion of years a connection occurs over of the 14-year period of summer 2005-2018. Darker colours indicate connections which occur regularly on a yearly basis. The 4 solid lines (2 vertical and 2 horizontal) represent 12.5º degrees of longitude divisions within the study domain, at -81.5º W and -69º W. Coloured cells below the dashed horizontal line represent transport towards the east, and coloured cells above the dashed horizontal line represent transport towards the west.

Unless otherwise stated, we report results on potential connectivity for the combination of larval behaviour 1, a 30-day pre-competency period and a summer larval release. The strongest larval dispersal pathways occurred southwestwardly between populations south of the Gulf of Maine (nodes #82-99), extending to north of Cape Hatteras (node #81, maximum connection probability of 16.11%) and within the western Gulf of Mexico (between nodes #1-16, maximum connection probability of 4.69%) (Figure 2.1; 2.2A-C; 2.3 A-C; 2.4A). Many, less probable, connections also occurred from populations on the western Florida shelf (nodes #17-31) to populations off eastern Florida (nodes #32-61) and eastern Florida north to Cape Hatteras (nodes #62-79, Figure 2.1; 2.2A-C; 2.3 A-C; 2.4A), which represent long distance dispersal and particle transport from the Gulf of Mexico to the eastern coast of the United States. This transport is captured with in-degree and out-degree (Figure 2.4C), the total unique incoming and outgoing connections for each node, respectively. Each of nodes #17-29 in the Gulf of Mexico form connections with 48-63 other nodes, and nodes #72-79 near Cape Hatteras each receive connections from 52-76 other nodes (Figure 2.1; 2.4C). Migration, which is the percentage of larvae arriving at a recipient population that originate at a specific source population, is also strong from populations in the eastern Gulf of Mexico to populations along the eastern coast of the United States. Specifically, nodes #28 and #29 are each responsible for more than 10% of the migration to 30 and 29 other nodes, respectively, and over 50% to 20 and 8 nodes, respectively (Figure 2.4B). These dominant connections are observed in all seasons (Figure 2.2A-C; 2.3 A-C) and are consistent across years (Figure 2.2D; 2.3 D).

Local retention was highest in the northern portion of the domain at The Gully and the *Lophelia* Coral Conservation Area (LCCA) at nodes #102-104, at 5.04%, 19.3% and 6.4%, respectively. There was also high overall retention within the Gulf of Mexico, as illustrated by the number of nodes that have high retention and the numerous bi-directional connections between nodes within the Gulf (lower left quadrant, Figure 2.2A-C; 2.3 A-C; 2.4D). The highest local retention in the GOM occurred at node #25 in the eastern Gulf at 8.56% and in the central Gulf at nodes #13 and #14 at 4.24% and 5.09%, respectively (Figure 2.4D). Strong local retention also occurred in the centre of the domain at Norfolk and Baltimore canyons (nodes #79, #80) at 4.77% and 4.78%, respectively. Areas of strong self-recruitment were spread throughout the domain with the highest at Baltimore Canyon (node #80, 91.48%), The Gully (node #103, 80.34%), the LCCA (node #104, 76.54%) and in the eastern Gulf at nodes #25 and #26 at 69.86% and 71.57%, respectively, possibly indicating greater isolation for these locations (Figure 2.4D). Local retention was higher throughout the domain for larval behaviour 1 than 2 and for a pre-competency period of 20-days than 30-days (Supplementary Figure A7).

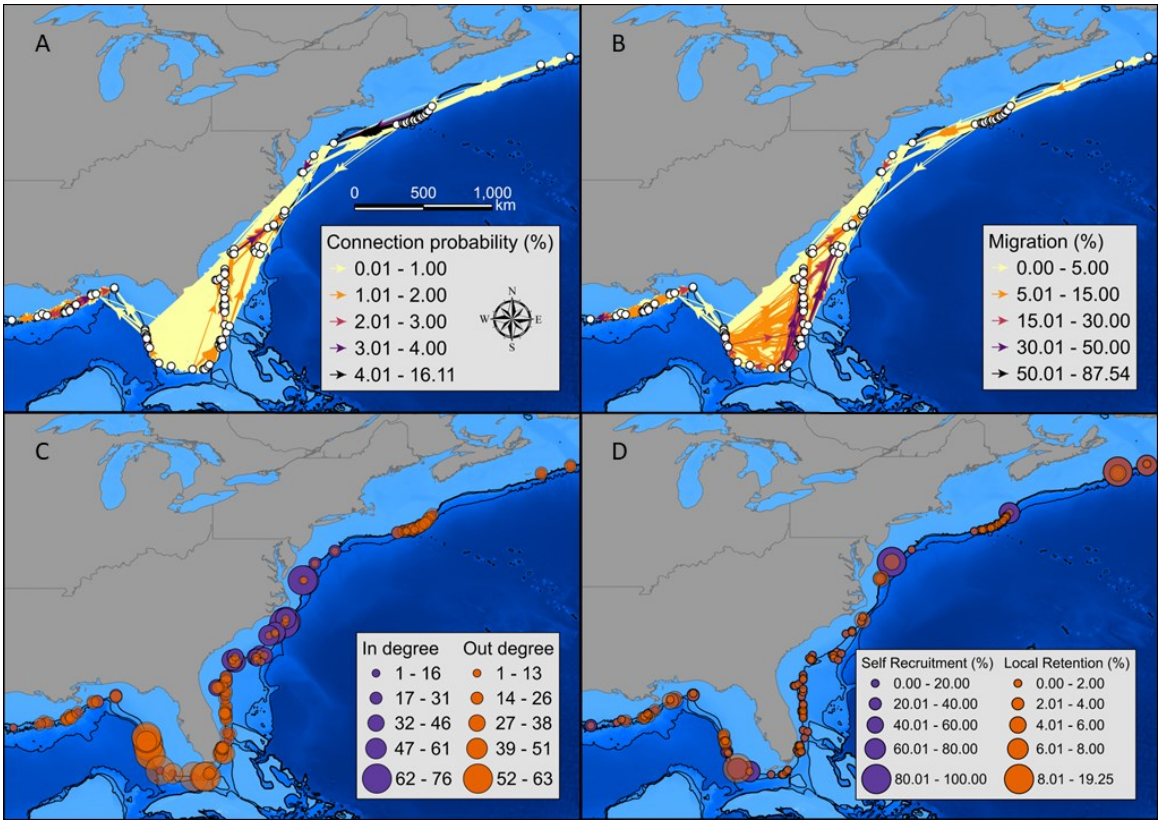

Figure 2.4 **A**- Connection probabilities, **B**- migration, **C**- in and out degree, **D**- self recruitment and local retention averaged over summer 2005-2018 for particles with a 30-day competency period and larval behaviour 1.

Betweenness centrality, which can be used to identify stepping-stones within a network, showed seasonal variability in strength. However, nodes in the Gulf of Mexico and in the center of the domain consistently scored the highest values, regardless of season (Figure 2.5A, C; Supplementary A6). For example, for nodes #12 and #16 in the central Gulf, and #17 and #18 in the eastern Gulf, between centrality was 361.96, 617.92, 317.68 and 345.71, respectively, whereas for nodes #44 and #72 in the center of the domain values were 395.01 and 299.91, respectively, in summer (Figure 2.1; 2.5A). The highest betweenness centrality scores occurred in autumn at nodes #12, #17 and #18

(603.51, 538.84 and 537.79, respectively), while maximum scores of 361.68 and 262.56 were reached at node #19 during winter and spring, respectively (Figure 2.5C, Supplementary A6). Google PageRank identified nodes off Cape Hatteras (# 75-79) as the most important for overall connectivity of the network, reaching a maximum score of 0.17 at node #78 in winter (Figure 2.5C). These nodes were consistently identified as the most important across all seasons (Supplementary Figure A8).

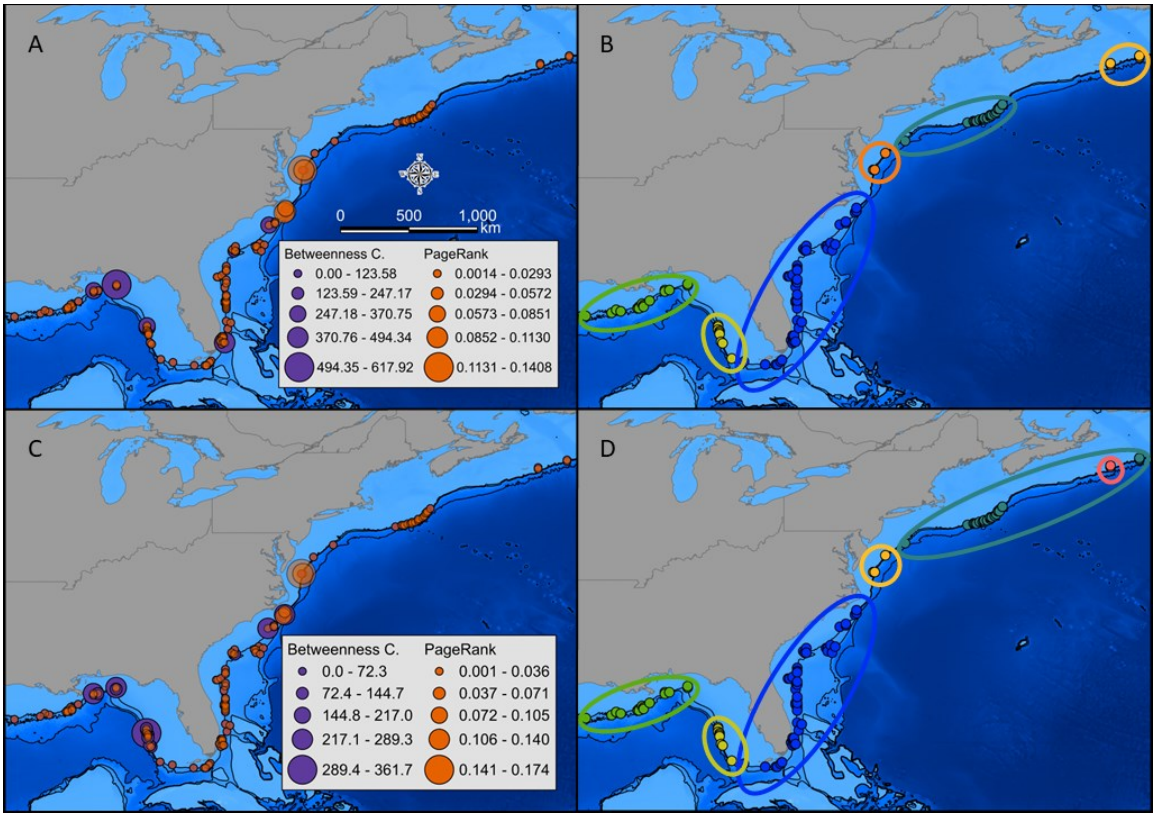

Figure 2.5– **A**- Betweenness centrality, Google Pagerank and **B** – cluster groupings identified through modularity clustering analysis averaged over summer 2005-2018 for particles with a 30-day pre-competency period. **C** – Betweeness centrality, Google PageRank for winter and **D** cluster groupings for Autumn averaged over 2005-2018 for particles with a 30-day pre-competency period. All panels for model runs with larval behaviour 1. Each colour in B and D denote a separate cluster.

A cluster grouping algorithm, which implements modularity to identify the most likely groupings of nodes based on connections between them, identified consistent clusters of nodes and modularity scores between dispersal simulations (Table 2.3). Six clusters were identified for dispersal with larval behaviour 1: two within the Gulf of Mexico, one extending from Florida north to Cape Hatteras, one north of Cape Hatteras to off Virginia, one from Virginia north to the Gulf of Maine and one in the northern most portion of the domain off Nova Scotia (Figure 2.5B, D). In autumn, the cluster off Virginia extended north to Nova Scotia and The Gully was identified as its own, separate, cluster. Modularity (Q) values ranged from 0.36 to 0.41 across all seasons and pre-competency periods (Table 2.3), indicating consistent, moderate structure within the network with many connections occurring between clusters. Seasonal variability in clusters was greater for the model run with larval behaviour 2, identifying 4-6 clusters depending on season and pre-competency period (Supplementary Figure A8). The spatial arrangement of clusters in the Gulf of Mexico were consistent across dispersal simulations, while clusters from Florida north to Cape Hatteras varied in their arrangement and overlap (Supplementary Figure A8).

2.5 Discussion

We uncovered three major patterns of connectivity among populations of *Lophelia pertusa* in the NW Atlantic and Gulf of Mexico: 1) strong connections exist between canyons on the continental slope off New England southwestwards towards Cape Hatteras; 2) extensive interconnections occur between the southwest Florida Slope (eastern Gulf of Mexico) and the southeastern United States (SEUS; eastern Florida to

Cape Hatteras); and 3) marked larval retention occurs within the Gulf of Mexico, Norfolk Canyon, and in the northern portion of the domain.

2.5.1 Seasonal and Interannual Variability

Seasonal and interannual variations in the observed patterns of connectivity were predominantly associated with low probability and sporadic connections. However, the dominant connection pathways and essential populations within the network remained unchanged across seasons, years, larval behaviours, and pre-competency periods. In contrast to other studies (Roughan et al. 2011; Treml et al. 2015), we illustrate that reproductive seasonality, larval swimming behaviour and duration of the pre-competency period may not be imperative for understanding potential larval connectivity pathways. Liu et al. (2021) found similar results when modelling larval dispersal for the deep-sea coral *Paramuricea biscaya* in the Gulf of Mexico, where a prevailing westward current dominates at depth, regardless of season. These findings also agree with regional-scale connectivity patterns for the deep-water sponge *Vazella pourtalesi* in the Western Atlantic which appear to be minimally influenced by any seasonal cycle (Wang et al. 2021).

The dominant concurrent influences of the Gulf Stream, Labrador and Nova Scotia currents, as well as the local Loop Current in the Gulf of Mexico, likely explain the seasonal and interannual consistency in connectivity within the NW Atlantic. Variability in the mean path and strength of the Gulf Stream is well documented (Rossby and Benway 2000; Bisagni et al. 2017; Seidov et al. 2019; Wang et al. 2022b). However, this variability is strongest after the Gulf Stream passes north of Cape Hatteras and would

predominantly affect larvae that travel far offshore with no opportunity to settle and form connections. The consistent flow direction of the Gulf Stream along the east coast likely explains the consistent connections, and the increased connection probabilities in summer may be explained by a peak in mean kinetic (Kang et al. 2016). Similarly, variability in the Labrador current and the Loop Current do not appear to influence our connectivity analysis (DeHaan and Sturges 2005; Peterson et al. 2017; Handmann et al. 2018). In contrast, seasonality and interannual variability may have stronger influences on connectivity in regions outside our domain. For example, in the NE Atlantic, larval dispersal and connectivity between populations of *L. pertusa* among MPAs was significantly altered by phase shifts in the North Atlantic Oscillation (NAO) on annual to decadal timescales (Fox et al. 2016).

2.5.2 Pre-competency period

We found that connectivity increased two-fold when pre-competency duration was reduced from 30 to 20 days, but the dominant pathways remained unchanged. The duration of the pre-competency period is influenced by environmental factors, such as temperature. Embryogenesis is accelerated at 11-12 °C compared to 7-8 °C, reducing pre-competency duration from 3 weeks to approximately 2 weeks (attributed to an increase in metabolic rate) (Strömberg and Larsson 2017). Relatively short distances between populations (10s to 100s of km) combined with strong regional currents facilitate rapid particle transport within the domain thus increasing the connection probability for larvae that reach settlement competency earlier. Due to the large range in environmental

conditions across our study domain, it is likely that larvae reach competency at different rates depending on their geographic location and depth. In the Gulf of Mexico, water temperature can vary by > 20°C from the seabed to the sea surface, but temperature differences throughout the water column may be much less pronounced in the northern portion of the domain, particularly in winter (DeHaan and Sturges 2005; Peterson et al. 2017). Therefore, the strength of the dominant connections will vary with pre-competency period, but the pre-competency duration is likely not constant across the domain.

2.5.3 Swimming velocity

We explored two different scenarios for larval behaviour in the model runs. Scenario 1, with larval swimming velocity increasing through ontogeny, resulted in increased connection probabilities, number of connections, local retention, and overall decreases in betweenness centrality and Google PageRank relative to Scenario 2. The initial low vertical swimming velocity after release resulted in larvae remaining closer to the seabed and experiencing slower currents for more of their PLD compared to larvae that swam at increased speeds throughout ontogeny (scenario 2). This behaviour reduced larval dispersion throughout the domain and strengthened connections with adjacent populations, thus reducing the importance of any population in the overall connectivity of the network. However, while scenario 1 increased connectivity, the overall patterns of connectivity (strongest connection pathways, important nodes, areas of retention) within the network remained largely unchanged compared with scenario 2, likely due to the consistent flow directions of the dominant currents.

2.5.4 Network Connectivity

The strongest (most probable) connections of the entire domain occurred with larvae originating from 18 populations between Welker Canyon and Corsair Canyon. These populations are located on the continental slope off New England, with larvae travelling southwestwards to canyons north of Cape Hatteras. Here *L. pertusa* occurs in high abundance, particularly in Kinlan Canyon (node #97) and Munson-Nygren Inter-canyon (node # 95) (162 and 65 coral presence records, respectively) and multiple presence records in the remaining 16 nodes. Colonies of *L. pertusa* collected from the Darwin Mounds, Therese Mount and South Porcupine Seabight in the NE Atlantic had an average fecundity of 3,146 (± 1,688) oocytes per polyp, and 3,300 oocytes per cm^2, or 99,800 oocytes for a colony around 30 cm^2 (Waller and Tyler 2005). While published values of fecundity in NW Atlantic populations of *L. pertusa* do not exist, if we assume that a healthy, reproductively mature colony would produce, at minimum, the quantity of oocytes released in this study (two orders of magnitude less than the fecundity recorded in the NE Atlantic), sufficient larval production to realize these strong, predicted connections is likely.

Middle Toms Canyon (node #81) was the primary recipient of larvae from the northern canyons off New England. Our data indicate that only six *L. pertusa* colonies have been observed in Middle Toms Canyon to date. These colonies appear healthy and occur at deeper depths (1483-1488 m) than the *L. pertusa* colonies found in other areas of our domain. Norfolk Canyon (nodes #78 and #79) also received larvae from the most northern canyons during our simulations and was consistently identified as a critical connectivity hub within the network by Google PageRank. Additionally, Norfolk Canyon

was one of the few locations north of Cape Hatteras to consistently receive larvae from the south as well as the north, thus suggesting that this canyon is the main node linking populations from north and south of Cape Hatteras. While Norfolk Canyon received larvae from many nodes to the north and to the south, these connections were predominantly of low connection probability (< 1%). The colonies observed in Norfolk Canyon appeared healthy and the abundance of suitable habitat (i.e. walls made of consolidated mud/ hard-packed clay) did not appear to be limiting the distribution of *L. pertusa* within the canyon (Brooke and Ross 2014). Middle Toms and Norfolk canyons have been protected since 2017 from bottom tending fishing gear under the Frank R Lautenberg Deep Sea Coral Protection Area (fisheries.noaa.gov, 2021).

Populations along the western Florida Slope, in the eastern Gulf of Mexico, were identified as critical to the supply of larvae to the eastern Florida Shelf north to Cape Hatteras by high out-degree and migration percentage. Particularly, node #28 at the south of the western Florida shelf (Pourtales Terrace - Brooke and Schroeder, 2007), was responsible for over 50% of the migration to 20 different nodes on the eastern Florida Shelf. The western Florida shelf is a gently sloping broad carbonate platform of authigenic carbonates (large plates, slabs, boulders and rubble) that provide hard substrate for abundant colonies of *L. pertusa* (406 observations in our dataset), including individual coral mounds 5 -15 m tall (Reed et al. 2006; Brooke and Schroeder 2007). Thus, multiple sections on the western Florida Shelf have been designated as Habitat Areas of Particular Concern (HAPC) and are protected from bottom-tending fishing activities (fisheries.noaa.gov, 2020).

High local retention could indicate multiple self-sustaining populations in the NW Atlantic (Lett et al. 2015). The highest local retention was observed in the most northern portion of the domain at The Gully and the LCCA. There was no larval input to The Gully or the LCCA from elsewhere in the domain in any of the dispersal simulations, suggesting that these populations can persist through local retention despite their isolation. Local retention is above average at both nodes within Norfolk Canyon and there is strong bi-directional connection probability between them, indicating a high percentage of larvae released at Norfolk Canyon stay within the canyon proper. High local retention was also observed within the Gulf of Mexico, although there appears to be a break between the central and eastern Gulf. In the central Gulf of Mexico, numerous, frequently occurring bi-directional connections were observed, with very little input from the east. However, this area is a hotspot for anthropogenic activity, particularly oil and gas extraction. Currently (as of August 1, 2023) there are 1,793 active oil and gas leases, covering over 9 million acres of seabed, in the Central Planning Area of the Gulf of Mexico (boem.gov, 2023). Physical disturbances to the seabed and oil spills related to mining can cause significant damage to the seabed and resident coral populations. Linkages from the eastern to central Gulf occur sporadically and with low probability thereby isolating the central region which could limit persistence and recovery post disturbance (Burgess et al. 2014).

2.5.5 Cluster Analysis

Overall, cluster analysis identified six consistent clusters of nodes in our domain: the central and eastern Gulf of Mexico, the Florida shelf north to Cape Hatteras, Cape

Hatteras north to Virginia, Virginia north to the Gulf of Maine, and one cluster in the northern most region of the domain off Nova Scotia. These clusters correspond well with the dominant currents, highlighting the importance of regional hydrodynamics in facilitating larval dispersal as well as acting as barriers to dispersal. These clusters also correspond to genetic patterns observed between the Gulf of Mexico and SEUS (Morrison et al. 2011). Our results of weak, somewhat frequent, long-distance dispersal with weak to moderate connectivity can help to explain the regional genetic cohesion within the Gulf of Mexico and within the SEUS, as well as genetic discontinuity between locations (Morrison et al. 2011). Interestingly, recent genetic analyses of *L. pertusa* colonies from Norfolk Canyon suggest that these colonies are more genetically similar to colonies in the Gulf of Mexico than to nearby colonies in canyons off New England or the SEUS (Weinnig et al. 2024 in review). In larval scenario 1, our simulations show a direct connection from the Gulf of Mexico to Norfolk Canyon is possible only in summer and at very low probability of occurrence (0.01%). In larval scenario 2, direct connections between the Gulf of Mexico and Norfolk Canyon are possible during all seasons at very low probability of occurrence (0.01%). The genetic similarity between these two locations suggests that these low probability connections are occurring or have occurred in the past. As local retention of larvae (this study) and rate of inbreeding (Weinnig et al. 2024 in review) is high within Norfolk Canyon, frequent incoming connections from the Gulf of Mexico are likely not required to sustain the population. Alternatively, there may be additional colonies of *L. pertusa* not accounted for in our modelling which act as stepping stone locations between the Gulf of Mexico and Norfolk Canyon. Our modelling suggests low-probability, infrequent larval interaction between

populations to the north and south of Cape Hatteras. In fact, northward larval movement did not occur past Middle Toms Canyon in any dispersal simulation. These results suggest that *L. pertusa* colonies in the Northern Domain were originally seeded through larval dispersal from NE Atlantic populations, which in turn would require a PLD of longer than 60 days to travel across the North Atlantic. This long PLD may be possible given the cold temperatures of the North Atlantic (Wisshak et al. 2005; Kenchington et al. 2017). Further biophysical modelling and genetic analysis of NW Atlantic populations are needed to explore this possibility.

2.5.6 Limitations

Our model utilizes the finest-scale data available in space and time for our entire target domain and given computational constraints. Finer-scale data could improve the accuracy of the modelling, particularly in areas of the domain where current flow is likely to be affected by bathymetric features, such as in canyons, which are coarsely resolved in the model. Additionally, it is difficult to accurately capture the realistic variation of the Gulf Stream in an ocean model without data assimilation. Hence, interpreting particle trajectories through the Gulf Stream must be done cautiously. A notable limitation to the BNAM model is that it does not include tidal influence, which will likely have a non-zero affect on dispersal, particularly in the Gulf of Maine. Further, it is likely that there are additional colonies of *L. pertusa* which have not been observed yet, and consequently not included in our model. The addition of newly located colonies to our model would not necessarily alter the connection pathways we have documented but would potentially

reveal new ones. In contrast, many of the observations are from the early 2000's, and these colonies may no longer exist due to natural death or from anthropogenic influences such as fishing and oil and gas extraction and could potentially remove certain connections. Combined, these limitations may result in discrepancies between our modelled potential connections and true larval connections in areas of complex fine scale-current flow, high tidal influence, and high anthropogenic impact.

2.5.7 Conclusions and Implications

Using biophysical modelling and graph theory to analyse connectivity patterns, we identify populations of the deep-water coral *L. pertusa* that are most essential for sustaining connectivity in the NW Atlantic. Our connectivity-based cluster analysis provides support for previous research suggesting well-mixed populations of *L. pertusa* within the Gulf of Mexico and Southeastern United States, and restricted geneflow between locations. Our observation of a possible pathway between the GOM and Norfolk Canyon, and high local retention at Norfolk Canyon also provide possible mechanisms for observed genetic trends. We showed a distinct break in connectivity between the SEUS and Northern Domain, providing support for a NE Atlantic origin for *L. pertusa* populations in the NW Atlantic. In contrast to previous studies, we found that spawning season, length of pre-competency period, and swimming velocity are not critical for understanding the dominant connectivity pathways in a deep-sea species. However, length of pre-competency period and swimming velocity do significantly affect the strength of the dominant connections. Our research has implications for conservation

by uncovering nuanced connectivity dynamics and highlighting isolated and potentially vulnerable populations of *L. pertusa.* This knowledge can offer valuable insight to managers seeking to incorporate connectivity information when designing protection zones focused on conserving *L. pertusa*. More broadly, our research provides support for incorporating connectivity information in deep-sea protection zones even when biological information on a species is limited or unknown.

Chapter 3

Climate change leads to disruptions in potential connectivity with minimal climate refugia for *Lophelia pertusa* (=*Desmophyllum pertusum*) in the Northwest Atlantic Ocean

3.1 Abstract

Climate change will cause loss of suitable habitat for many marine species, resulting in local extinctions, removal of subpopulations and disruption of population connectivity. However, species ranges can also expand with previously unsuitable habitat becoming suitable. For sessile benthic invertebrates, larval dispersal provides the main mechanism for habitat and population connectivity. Biophysical modelling of larval dispersal can be used to quantify dispersal pathways, and when combined with graph theory analysis elucidate potential connections between populations, evaluating their importance to the stability of the entire network. We use a predictive habitat suitability model for 2081-2100 to simulate habitat loss for the deep-water coral *Lophelia pertusa* (=*Desmophyllum pertusum*) over its range in the Northwest Atlantic Ocean. After removing habitat areas predicted to become unsuitable, we simulated larval dispersal for *L. pertusa* using a high-resolution ocean circulation model. Then, using present-day and future habitat suitability models, we identified areas which could potentially act as climate refugia for *L. pertusa* in the NW Atlantic, and simulated larval dispersal in reverse to identify potential larval sources for these refugia. Habitat loss was greater in the Gulf of Mexico (GOM) and Southeast United States (SEUS) than in the northern regions of the domain. Bi-directional larval transport between the SEUS and the Northern Domain, and migration from the GOM to the SEUS ceased after 20% and 60% habitat loss, respectively. Strong local retention and connections in the Northern Domain remained throughout the habitat loss simulation, suggesting these populations may be more likely to persist in the face of climate change compared with GOM and SEUS. Potential climate change refugia were numerous in the Northern Domain, extending further north than current *L. pertusa* records. However, our analyses suggest that larval connectivity to these refugia is unlikely under our modelling parameters. Our results highlight the potential for drastic changes to connectivity in a deep-sea species due to habitat loss, and the importance of considering larval dispersal when assessing the potential for species to colonize newly available habitat.

3.2 Introduction

Climate change is unambiguous and is causing increased ocean temperatures, ocean acidification, and deoxygenation which have significant impacts on marine life, from phytoplankton to fish to marine mammals (Beaugrand 2009; Poloczanska et al. 2013; Zheng and Cao 2014; Pinsky et al. 2019). Climate-related changes in the ocean vary with geographic location, latitude, and depth, but extend throughout the water column from the surface to the deep ocean (Sweetman et al. 2017; Brito-Morales et al. 2020). The severity of impacts on organisms will depend on their ability to adapt to new conditions, whether through range shifts to new habitat, or organismal adaptation to more extreme conditions in situ (Burrows et al. 2011; Poloczanska et al. 2013; Gunderson and Stillman 2015). Range shifts result from expansion into areas that were previously unfavourable and will relate to an organism's traits of dispersal and recruitment (Sunday et al. 2012).

The Northwest Atlantic ocean is considered a climate change hotspot and associated impacts are expected to be significant on numerous species including fishes and invertebrates (Hiddink et al. 2014; Stanley et al. 2018; Morato et al. 2020). For marine benthic invertebrates, a response to climate driven oceanographic changes is challenging because of their limited motility as adults (Hiddink et al. 2014). Benthic invertebrates predominantly rely on larval dispersal to colonize new habitats which is grossly determined by local current regimes (Pineda et al. 2007). This can lead to local extinctions at the contracting edge of habitat ranges (Wiens 2016).

For the structure forming deep-water coral, *Lophelia pertusa* (= *Desmophyllum pertusum*)[2], suitable habitat in the North Atlantic Ocean is predicted to decrease by 79% by 2081-2100 under RCP 8.5 or business-as-usual scenario (Morato et al. 2020). *Lophelia pertusa* is currently found at temperatures ranging from 4 to14°C, depths from 200 meters to over 1,000 meters, and areas of moderate current velocities (Pires et al. 2014; Brooke and Ross 2014; Ross et al. 2015; Kenchington et al. 2017; Sundahl et al. 2020; Tong et al. 2022). The pronounced reduction in suitable habitat for *L. pertusa* is primarily linked to increasing ocean temperatures above its thermal maximum. However, the projected decrease in suitable habitat is not uniform throughout the North Atlantic Ocean, being greater at low latitude areas than high latitude areas; some expansion of suitable habitat further north is predicted. As temperatures increase, areas such as the Davis Strait and Labrador Sea, as well as areas deeper on the continental slope, are predicted to become more suitable than in present day (Morato et al. 2020).

For newly available suitable habitat to provide refuge for *L. pertusa* from changing ocean conditions, larval connections from existing populations must be present. Increasing temperature can also affect life-history traits, such as rates of larval development, and may influence spawning times (Strömberg and Larsson 2017). The warming of the deep ocean may therefore lead to increases in metabolic rate and increases in larval development rates. Increases in metabolic and development rates can lead to decreases in Pelagic Larval Duration (PLD), potentially limiting the dispersal

[2] A taxonomic change from *L. pertusa* to *D. pertusum* has been proposed (Addamo et al. 2016) and now accepted in the World Register of Marine Species (WoRMS) database (Hoeksema and Cairns 2023). However, we agree with Dr. Steve Cairns (WoRMS database editor) to exercise caution in changing nomenclature until more research is done and elect to use the older nomenclature herein.

potential of larvae (O'Connor et al. 2007; Larsson et al. 2014; Strömberg and Larsson 2017) and ability to colonize new habitats.

By integrating biological processes, such as spawning season, larval development, mortality, and behavior, with physical factors such as ocean currents, temperature, and salinity, biophysical models can predict patterns in larval dispersal and thus potential connectivity (Connolly and Baird 2010; Cardona et al. 2016; Assis et al. 2021). Using these predictions, graph theory can be used to create network models that represent real world metapopulations and quantify the importance of nodes and connections within the network (Cecino and Treml 2021). Predictive habitat suitability models combined with network models can be used to assess changes to potential network connectivity after habitat loss.

In this study, we simulate the sequential elimination of *L. pertusa* populations (i.e. nodes) in the NW Atlantic ocean (from the Gulf of Mexico to the Laurentian Channel), based on predicted major declines in suitable habitat for 2081-2100 under RCP 8.5 (Morato et al. 2020). After removing populations in areas of degraded habitat, we conducted larval dispersal simulations to determine effects of removal on present day dispersal pathways and connections (as identified from Chapter 2). Using graph theory, we also determine the effects on connectivity metrics, such as out-degree, in-degree, local retention, self-recruitment, and Google PageRank. Lastly, we identified areas of current suitable habitat (1950-2000) which overlap with areas of predicted future suitable habitat (2081-2100), to detect potential climate refugia for *L. pertusa*. Using biophysical modelling to simulate reverse larval dispersal from these climate refugia, we identified potential source locations of larvae, and determined whether connections between

existing populations and newly identified climate refugia are possible. Such knowledge is critical to understanding how metapopulation connectivity will be affected by climate change, and when assessing the potential for a species to colonize new habitat predicted to become suitable in a changing ocean.

3.3 Methods

3.3.1 Data collection

We assembled presence records of *L. pertusa* from several sources including video surveys by Remotely Operated Vehicle (ROV) on the NOAA ship *Okeanos Explorer* during the research cruise EX1905 (2019), ROV video and trawl surveys performed by Fisheries and Oceans, Canada (DFO) on the *CCGS Hudson* (2003-2018), NOAA's Deep-Sea Coral Data Portal (1968-2019), and Martha Nizinski (NOAA, ROV video and towed-camera imagery 2012-2017) (for details see Ch. 2) (Supplementary table A1). We used 3780, highly clustered, observations of individual colonies of *L. pertusa*, which we aggregated over a 0.1^{o}x0.1^{o} spatial grid, in turn assigning *L. pertusa* to 103 grid cells in the domain.

3.3.2 Study Domain

The domain was restricted to the Northwest Atlantic, spanning from within the Gulf of Mexico in the southwest to the eastern Scotian Shelf at the northeast boundary (Figure 2.1). The region is dominated by two energetic western boundary currents in the North Atlantic Ocean - the Gulf Stream and Labrador Current, and an on-shelf current – the

Nova Scotia Current. The warm northward travelling Gulf Stream exits the Gulf of Mexico and travels north along the shelf break before separating from the continental shelf near Cape Hatteras, North Carolina, and then advances eastwards towards the Grand Banks, forming complex meandering eddies (Rossby et al. 1985; Rossby and Benway 2000; Bisagni et al. 2017; Seidov et al. 2019). The cold Labrador Current originates in high latitudes in the north and flows equatorward along the shelf break. A confluence zone between the Gulf Stream and the Labrador Current forms in the off-shelf region (Han et al. 2010) (Figure 2.1). The Nova Scotia Current originates in the Gulf of St. Lawrence and enters the Scotian Shelf through the Cabot Strait, flowing on the Scotia Shelf into the Gulf of Maine, where it forms a counterclockwise mean circulation (Townsend et al. 2006). The upper 800-1000 m in the Gulf of Mexico are dominated by the anticyclonic Loop Current (LC) which flows clockwise around the basin from the Yucatan Channel to the Florida Straights, with anticyclonic mean near-bottom circulation (DeHaan and Sturges 2005).

3.3.3 Dispersal Simulation

We extracted 3-D hydrodynamic currents of the North Atlantic Ocean from the eddy resolving BNAM (Bedford Institute of Oceanography North Atlantic Model), which is based on version 2.3 of NEMO (Nucleus for European Modelling of the Ocean), a framework for ocean modelling (https://www.nemo-ocean.eu/.). BNAM covers the entire North Atlantic Ocean, with grid sizes of 2.7 km (zonal direction) and 2.1 km (meridional direction) in the northernmost part of the domain and increases to a maximum of 9.17 km

at the southern boundary of the domain. There are 50 vertical layers, varying in thickness from 1 m at the surface to 450 m at the seabed. BNAM currents have been ground-truthed and agree well with the surface currents derived from surface drifter data and bottom currents from current meter data (Wang et al. 2018). Monthly-mean current data were extracted for 2005 -2018 from BNAM for the spatial domain bounded by the 60º-17ºN parallels and 48º-95ºW meridians.

We ran 3-D particle tracking simulations using OceanParcels v2.4.0 Lagrangian Framework (Delandmeter and van Sebille 2019) on the ocean circulation data extracted from BNAM. Simulated particles were advected in the Parcels framework using the fourth order Runge-Kutta method. Each 0.1ºx0.1º grid cell containing *L. pertusa* was seeded with particles at an equal spacing of 0.003º (see Ch. 2 for justification) which equalled 1156 particles per cell, for a total of 119,068 particles over the entire domain. We ran the model in forecast mode using monthly mean currents, and tracked particles released on the 1st day of each month from January 2005 to December 2018 and condensed the monthly model outputs by averaging over 2005-2018 to produce mean long-term dispersal. We included random horizontal particle movement in the model to simulate ocean processes not resolved by the model, using a horizontal diffusivity constant, K_h (cm^2s^{-1}), with the scale of diffusion depending on the spatial resolution of the ocean model (BNAM), which varies with latitude over the study domain (Ch. 2, Wang et al. 2022). K_h values were calculated for each grid cell, and varied from 25.86 m^2s^{-1}, in the north, to 91.88 m^2s^{-1}, in the south.

We included several biological parameters in the model, selected based on results in Ch. 2. Vertical swimming velocity was directed towards the surface during the pre-

competency period and altered to bottom-probing behaviour once larvae reached competency. The pre-competency period was set to 30 days and velocity increased linearly from 0 mms^{-1} on day 0 to a maximum of 0.88 mms^{-1} at the end of the PLD (Strömberg and Larsson 2017).

3.3.4 Sequential removal of nodes, simulating habitat loss

A habitat suitability (HS) model for *L. pertusa* in the North Atlantic from 2080-2100 at RCP 8.5 (business-as-usual scenario) (Morato et al. 2020) was used to determine the degree of HS at identified nodes (see Ch. 2) during predicted future conditions. Morato et al. (2020) used an ensemble modelling approach, including maximum entropy modelling, generalized additive modelling, and random forest machine learning algorithms – all capable of dealing with presence-only data with pseudo absences. Environmental variables for future conditions were downloaded from the Earth System Grid Federation (ESGF) Peer-to-Peer enterprise system (https://aims2.llnl.gov/search). A detailed description of the HS model can be found in Morato et al. (2020).

The future habitat suitability output was overlaid on the 103 grid cells identified as source locations in Ch. 2. To extract a single HS value for each 0.1ºx0.1º source cell, we averaged HS values at all *L. pertusa* observation within each source cell. The nodes (cells) were then ranked from most suitable to least suitable during predicted future conditions. The least suitable nodes were systematically removed in 10% intervals starting with the least suitable 10%, which resulted in ~10 nodes being removed at each iteration (Figure 3.1).

3.3.5 Network Analysis

To estimate connectivity from the particle trajectories, we calculated probability matrices, (see details in Ch. 2). We defined connection probability as the number of particles which travel from source cell *j* to receiving cell *i*, divided by the number of particles released at source cell *j*. We calculated mean connection probability for the period of 2005-2018.

For the network analysis, the domain was divided into three separate geographic areas: the Gulf of Mexico (nodes #1-31), the South-east United States (nodes #32-81) and the northern domain (nodes #82-103) (Figure 3.1). After each node-removal iteration, we applied graph theory to quantify relationships between source and receiving cells, to calculate connectivity metrics and to detect communities of *L. pertusa* within the network. We selected 2 indices of self persistence (ability of a local population to persist independently of input from other populations within the network): local retention (LR) and self-recruitment (SR). We also included 3 measures of centrality (which identify the most important nodes within a network by evaluating their connection strength and the number of connections with other nodes: in-degree (ID), out-degree (OD), and Google PageRank (PR) (Table 2.2).

Communities were detected using the Leiden algorithm which assigns individual nodes to communities based on the number of connections between those nodes (i.e. communities are groups of nodes which have a high number of connections between them) (Traag et al. 2019) (see Ch. 2 for details). To assess the strength of the community divisions, we used the benefit function, *Q*, a measure of how confidently a graph can be

separated into communities. Q ranges from 0 for a completely random graph to 1 for a graph with a high number of connections within communities and minimal connections between communities (Leicht and Newman 2008).

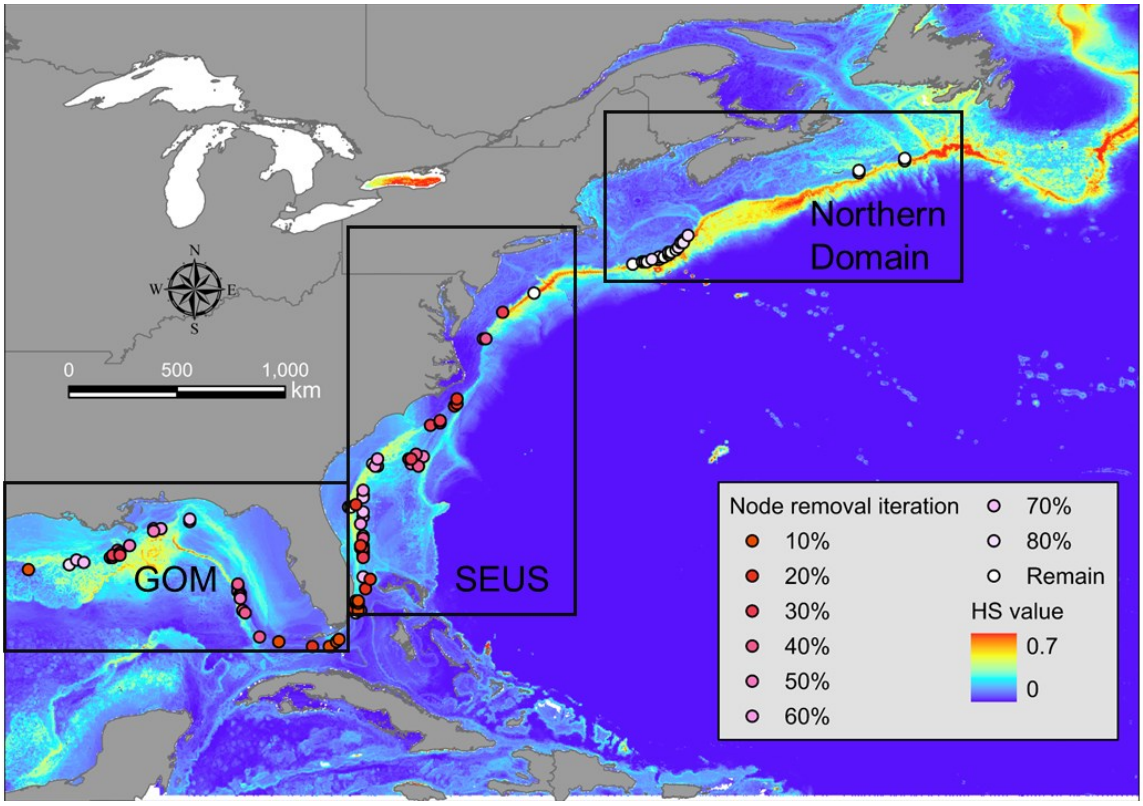

Figure 3.1 Map of the domain included in the study with habitat suitability for 2081-2100 under RCP 8.5 or business as usual scenario from Morato et al. (2020). Points show source locations of *L. pertusa* from Chapter 2 coloured based on which iteration they were removed. Darker reds were removed at earlier iterations than lighter reds and white points remained after 80% of nodes were removed. Black boxes identify the three regions in which the domain was divided for the graph theory analysis after each node-removal iteration.

3.3.6 Reverse Simulation of Dispersal

The future habitat suitability output was combined with a present-day (1951-2000) habitat suitability output (Morato et al. 2020) to select locations that could potentially act as climate refugia. We used a 0.1^{o}x0.1^{o} grid overlain on both the present-day and future habitat suitability outputs to select locations where HS was predicted to be ≥ 0.3 in both timeframes. This identified 265 locations with habitat suitability ≥ 0.3 in present and future scenarios (Figure 3.2). We chose HS ≥ 0.3 as a trade off between representing suitable habitat and still including a suitable number of nodes in the analysis (i.e. using HS ≥ 0.4 resulted in only 4 possible locations).

From each of the 265 locations, particles were released on the first day of each month (January-December) for a single randomly chosen year (2010) and tracked in reverse for 60 days to identify potential source populations which could colonize climate refugia. Results from these 12 monthly model outputs were averaged to produce a single particle density distribution and average dispersal tracks for the year. The domain was expanded to the south to include 2 additional potential source populations off Puerto Rico.

Choosing locations suitable under both present and future conditions was deemed necessary as our ocean circulation data is for present day (2005-2018) and does not include predictions on future circulation conditions. Thus, we sought to identify locations which could be colonized through larval dispersal under present ocean circulation conditions and would remain viable for coral colony survival into the future.

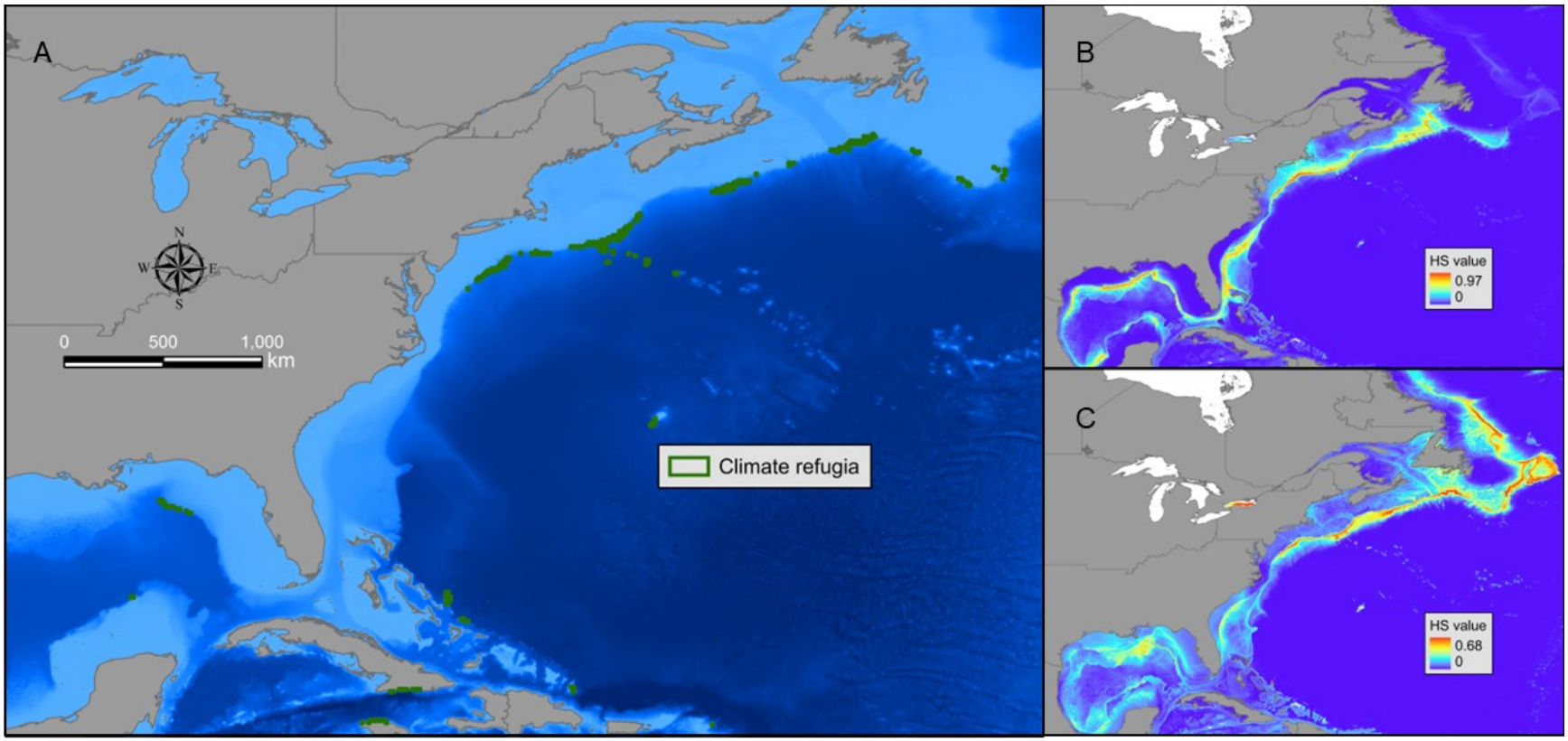

Figure 3.2 **A** – climate refugia (265) identified as overlapping locations in both **B** - present-day (1951-2000) and **C** - future (2081-2100) habitat suitability for *L. pertusa* in the NW Atlantic (Morato et al. 2020) with values ≥ 0.3.

3.4 Results

Nodes in the Gulf of Mexico (GOM) and Southeast United States (SEUS) were removed earlier than those in the Northern Domain, due to larger declines in suitable habitat in those regions (Figure 3.1). After removing 80% of the nodes from the network based on lack of suitable habitat, the number of nodes in the GOM decreased from 31 to 0, in the SEUS from 50 to 4, and the Northern Domain from 22 to 16 (Figure 3.1). Every node in the Northern Domain remained until 80% of the nodes were removed from the network.

3.4.1 Connectivity metrics

In the GOM, in- and out- degree decreased linearly from 17.5 and 37.6, respectively, to 0 after 80% of the nodes were removed. Local retention increased initially, from 2.1% to 2.6% after 50% node removal, then decreased sharply to 0%. Self-recruitment increased as nodes were removed, from 17.3% to 100% after 70% node removal, and dropped to 0% at 80% node removal (Figure 3.3 A, B).

In SEUS, in- and out- degree decreased linearly from 33.1 and 18.4, respectively, to 11.5 and 1.75 after 80% node removal. Local retention increased initially, before falling sharply from 0.98% to 0.06% after 40% node removal. Self-recruitment decreased from 7.5% to 4.6% after 70% node removal and increased to 39% after 80% node removal (Figure 3.3 C, D).

In the Northern Domain, local retention, self-recruitment, and in-degree remained unchanged after 70% node removal and out-degree decreased from 19.5 to 16.4 between 10% and 40% node removal, after which it remained unchanged until 80% node removal. After 80% node removal, in and outdegree decreased from 15.4 and 16.4 to 12.1 and 13.1, respectively. Self-recruitment and local retention increased from 12.8% and 1.5% to 14.8% and 1.9%, respectively (Figure 3.3 E, F).

Google PageRank values at Norfolk Canyon (node #79 and #80) increased initially as nodes were removed from the network, before being lost at 40% node removal. Subsequently, the dominant node was identified further to the north at Middle Toms Canyon, the PR values of which increased as nodes were being removed (Figure 3.4). Most nodes in the network had low PR scores which remained low as nodes were removed.

Modularity (Q) values increased from 0.32 to 0.45 after 40% node removal, then decreased to 0.12 after 80% removal, with the number of clusters ranging between 4 and 6 (Figure 3.3 G).

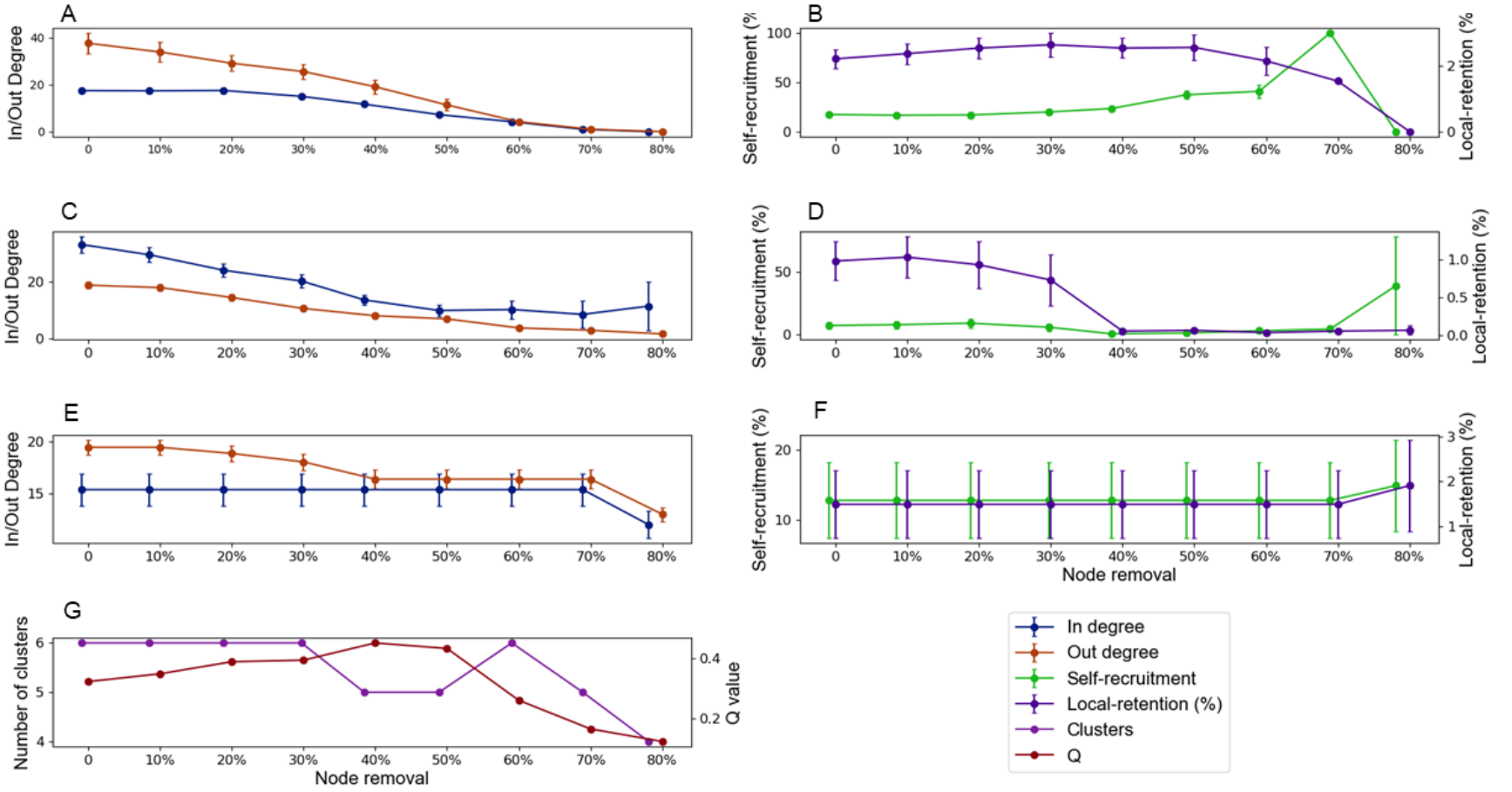

Figure 3.3 In- and out-degree, self-recruitment (SR) and local retention (LR) for **A**/**B**– Gulf of Mexico, **C**/**D** – Southeast United States and **E**/**F** – Northern Domain after each node-removal iteration. Error bars represent standard error of the mean (SEM). **G** – Modularity (*Q*) values and the number of clusters identified after each node-removal iteration.

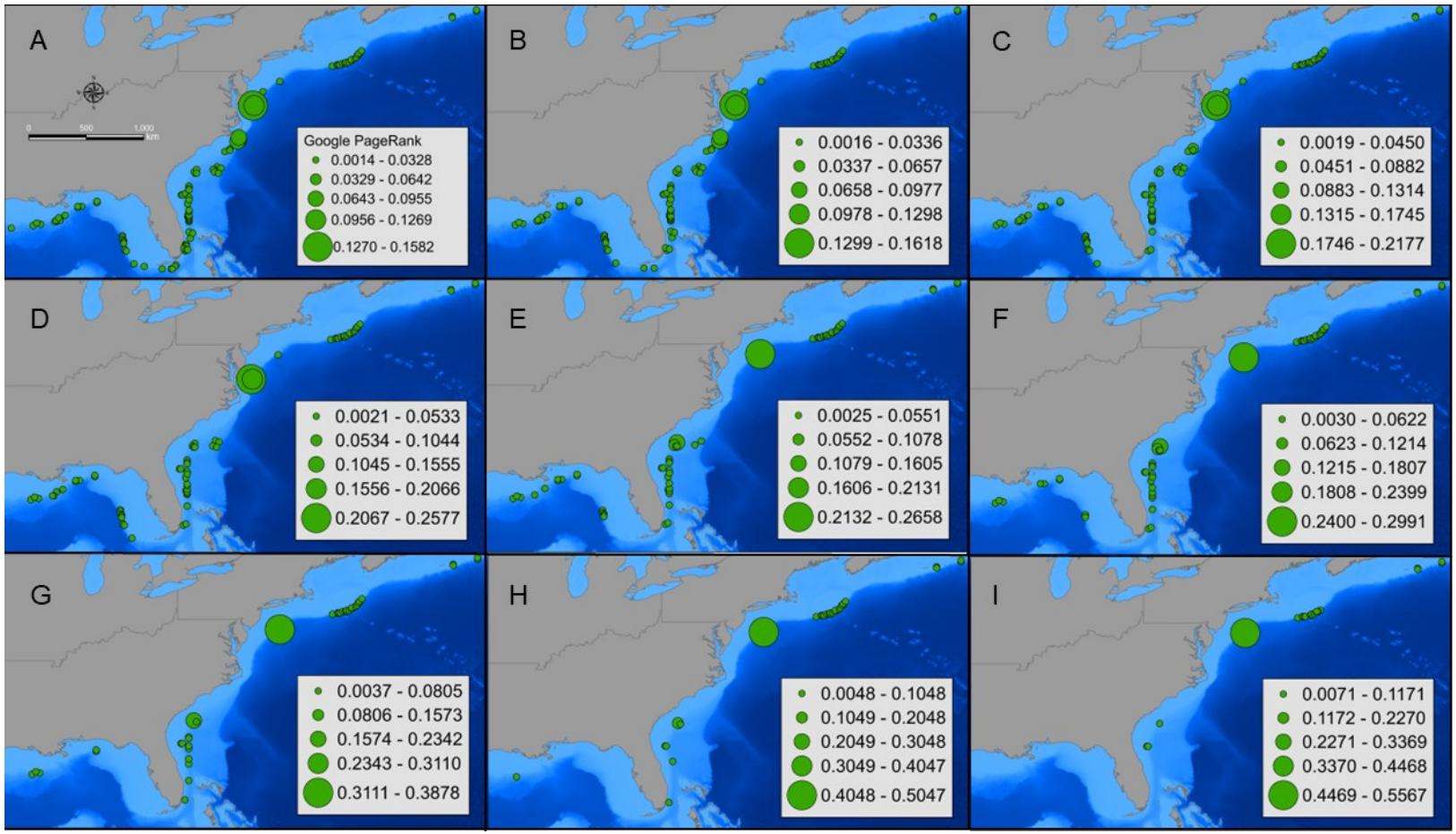

Figure 3.4 Google PageRank values for each node-removal iteration from **A** - original (no nodes removed) to **I** – 80% of nodes removed.

3.4.2 Reverse Simulation of Dispersal

Most (76%) climate change refugia were identified to the north of Norfolk Canyon and 42% were concentrated in canyons and on seamounts off New England (Figure 3.2). Significant refugia were also identified on the continental slope off the central Scotian Shelf and to the south of Newfoundland. Climate refugia were also present in the GOM, off Cuba, Jamaica, the Bahamas, Puerto Rico, and Bermuda (Figure 3.2).

Large numbers of particles capable of reaching potential climate refugia originate offshore in the NE Atlantic (Figure 3.5). In the Northern Domain, potential sources of particles were concentrated along the Scotian Shelf and slope and surrounding the Grand Banks. The strongest possible connections from current *L. pertusa* populations to climate refugia appeared in the Northern Domain (4-5% connection probability), from nodes off New England (#81-96) to suitable habitat off Virginia (Figure 3.6). Climate refugia off the Scotian shelf could receive substantial larval input from both The Gully and LCCCA. There is little evidence of larval sources to climate refugia northeast of the LCCA (Figure 3.6).

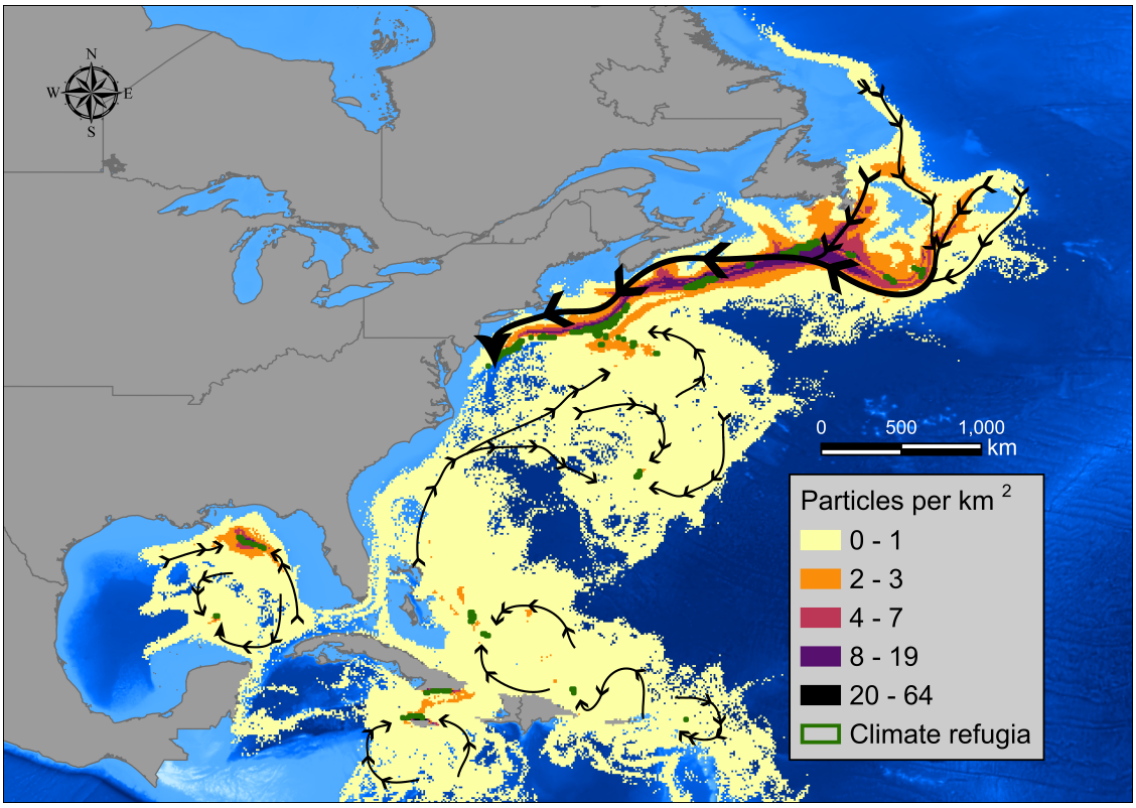

Figure 3.5 Mean particle density distribution for particles released from climate refugia (green squares) and tracked in reverse for 60 days to identify potential source populations. Direction and width of the black arrows show direction and relative magnitude of particle transport.

Sources of particles adjacent to the SEUS were dispersed, with many originating from offshore areas (Figure 3.5). Larvae from SEUS populations can seed climate refugia surrounding Bermuda, albeit at low probabilities (< 0.5%). Climate refugia at NE Seamounts also have a low probability of being reached from NE canyons and the populations at SEUS. No connections were observed between *L. pertusa* populations and potential climate refugia off Cuba, Jamaica, the Bahamas, or in the central GOM (Figure 3.6).

In the northern GOM, sources of particles capable of reaching the climate refugia are densest directly surrounding the climate refugia (Figure 3.5). The strongest connections

(1.5-2.5%) to these refugia come from the Central GOM (nodes #1-10), as well as less probable connections from the western Florida shelf. Climate refugia near Puerto Rico can also be reached by larvae from nearby *L. pertusa* populations (Figure 3.6).

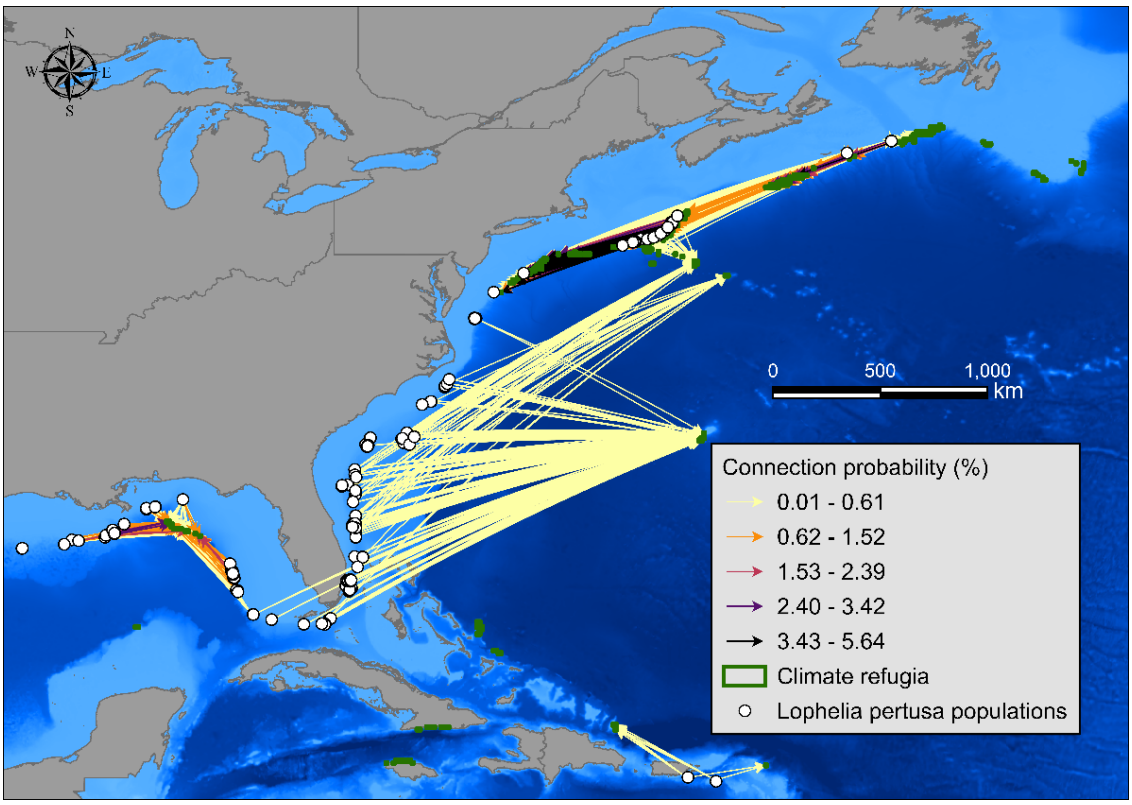

Figure 3.6 Potential connections between *L. pertusa* source populations (Ch.2) and potential climate refugia.

3.5 Discussion

Suitable habitat at all *L. pertusa* populations (i.e. nodes) throughout the network is predicted to decrease by 75% for the period 2081-2100 compared to 1951-2000 (compared to 79% predicted decline for the whole North Atlantic Ocean). However,

nodes in the GOM and the SEUS reach lower overall habitat suitability (HS) scores for the period 2081-2100 compared with those in the Northern Domain. The decline in suitable habitat for *L. pertusa* in the NW Atlantic is primarily linked to the anticipated warming of deep waters (Morato et al. 2020). Seafloor temperatures in the GOM and SEUS are projected to increase at a greater rate than those on the Scotian Shelf and Slope, and south of the Grand Banks (Sweetman et al. 2017). *Lophelia pertusa* has a temperature preference of 4-14 ºC and experiences significant mortality when exposed to temperatures above 14 ºC for several weeks at a time (Brooke et al. 2013; Lunden et al. 2014). In areas of the GOM and SEUS, *L. pertusa* may be currently occupying areas close to its thermal maximum, particularly in summer, possibly increasing its susceptibility to prolonged fluctuations in temperature (Reed et al. 2006; Mienis et al. 2012).

In some cases, the persistence of an entire metapopulation may depend on the functionality of a single critical link (Artzy-Randrup and Stone 2010). For *L. pertusa* in the NW Atlantic, this critical link may be the subpopulations surrounding Cape Hatteras, at Cape Fear and Cape Lookout to the south, and at Norfolk and Middle Toms Canyons to the north. This region facilitates connections between the north and south of Cape Hatteras and is identified by PageRank as an important grouping of nodes in the network. Populations at Cape Fear and Cape Lookout are lost early in our analyses due to severe decreases in suitable habitat. The removal of Cape Fear and Cape Lookout halts bi-directional larval exchange between south and north of Cape Hatteras, effectively separating larval interaction between the SEUS and the Northern Domain. Converging currents at Cape Hatteras create a known biogeographic boundary for species in the

subtidal zone (0-100m depth) (Savidge and Bane 2001; Pappalardo et al. 2015; Krumhansl et al. 2023). Our results suggest that this boundary affects deep-sea species as well, and that climate-change caused habitat loss may strengthen this boundary and contribute to increased biogeographic separation of the two regions. Numerous processes, such as oceanographic currents, thermal extremes, biological interactions and habitat distribution can all affect the location of biogeographic boundaries (Parmesan et al. 2005). The depth distribution of a species can influence how it is affected by a certain boundary (Pappalardo et al. 2015), and a better understanding of how these processes affect larval dispersal in deep-sea species will be imperative to predicting the distribution of deep-sea species in response to climate change.

Metapopulation persistence depends on larval dispersal (connections) between subpopulations, larval retention at natal sites, as well as successful recruitment into populations (Bode et al. 2008; Lett et al. 2015; Treml et al. 2015). As metapopulations become more fractured and connections between subpopulations less probable, individual subpopulations may increasingly depend on local retention for self-persistence. High local retention reduces the dependence of an individual subpopulation on larval input from other populations (Hogan et al. 2012). In the GOM, a continuous increase in self-recruitment throughout simulated habitat loss emphasizes that nodes are becoming increasingly more isolated and rely more heavily on local retention for persistence. Self-persistence through local retention is conceivable. An increase in local retention, up to the removal of 50% of the habitat, indicates that nodes with high local retention are being preserved over nodes with low local retention. Thus, some populations in the GOM may

be able to sustain themselves through local retention until a large percentage (> 50%) of suitable habitat is lost.

The number of local out-going connections has been found to have the largest impact on metapopulation persistence, as nodes with high out-degree are important sources of larvae to neighbouring populations (Cecino and Treml 2021). The number of out-going connections between domain sections decreases steadily as habitat is removed, leading to increasing isolation. Notably, nodes on the western Florida Slope, which have low predicted future habitat suitability and support high migration to SEUS populations (Ch. 2), are removed early on in our analyses. Colonies on the western Florida Slope are primarily responsible for out-going connections to the SEUS. If habitat on the western Florida Slope becomes unsuitable and *L. pertusa* becomes locally extinct, the SEUS is cut off from incoming connections from the GOM. In contrast, the Northern Domain is relatively stable throughout the habitat loss simulations, and out-degree remains high. As mentioned, out-going connections form the Northern domain to Cape Fear and Cape Lookout are lost, however, all other connections within the Northern Domain remain. Due to the asymmetry of the network, the Northern Domain does not appear to rely on SEUS populations as larval sources, and the major habitat losses in the SEUS have little impact the connectivity within the Northern Domain.

3.5.1 Climate refugia

Potential climate refugia were predominantly identified in the Northern Domain near existing colonies (but at deeper depths), and extending further to the north, south of

Newfoundland. The absence of any climate refugia identified in the SEUS could be a result of our chosen future species distribution model. The future habitat distribution model by (Morato et al. 2020) evaluates the decline in suitable habitat at existing populations and identifies climate refugia based on RCP 8.5 or 'business-as-usual' scenario. If commitments to reduce greenhouse gas emissions are implemented completely and on time, then it is hopeful that climate-change related declines in suitable habitat will be less severe than predicted under RCP 8.5 (Meinshausen et al. 2022). Gasbarro et al. (2022) utilized modeled climate data based on intermediate emission pathways, Shared Socioeconomic Pathways 2 (SSPs) - 4.5 and SSP3 - 7.0, to estimate future habitat suitability for *L. pertusa* in the SEUS region and found less decline in suitable habitat for *L. pertusa* on the Blake Plateau. They suggest the eastern Blake Plateau could serve as critical climate refugia, which was not identified using our methods.

3.5.2 Identification of potential source populations for climate refugia

Poleward range shifts for species affected by changing ocean conditions have been documented for numerous species (Burrows et al. 2011; Pinsky et al. 2019, 2020). The northward expansion of suitable habitat and potential climate refugia for *L. pertusa* in the NW Atlantic suggests the possibility that metapopulation equilibrium could be sustained by establishing new subpopulations in recently suitable poleward habitats, thereby compensating for the loss of subpopulations to the south (Hanski 1999). However, due to the predominant equatorward direction of the Labrador Current, it appears unlikely that

larvae originating from colonies in the Northern Domain can travel northward to reach the climate refugia south of Newfoundland or the predicted future suitable habitat further north. In our analyses, refugia at the mouth of the Laurentian Channel are the furthest north to receive connections (albeit with low probability) from existing colonies to the south. The simulated larvae which can reach the climate refugia south of Newfoundland originate from regions surrounding the Grand Banks and off the coast of Labrador. There are no records of *L. pertusa* in these areas, and the nearest documented colony to the north is from Greenland (Kenchington et al. 2017). Connection between the Greenland colony and climate refugia south of Newfoundland is not possible using our model parameters. However, this connection becomes possible when the PLD is increased from 60 to 180 days. *Lophelia pertusa* larvae have survived for a full year in laboratory settings (Strömberg and Larsson 2017), and it is suggested that the maximum lifespan could be even longer. Therefore, it seems likely that northern climate refugia will need to rely on larval colonization from populations in the NE Atlantic, if possible. Asymmetric larval movement has been previously identified in the NW Atlantic and it has been suggested that there is limited potential for temperate to subarctic larval exchange on the east coast of Canada (Pappalardo et al. 2015; Krumhansl et al. 2023), also in agreement with our findings. Our results substantiate the importance of considering local current regimes when assessing potential range expansions for species with a prevalent larval stage, which could more accurately predict a species range than solely using environmental parameters, such as temperature (Pappalardo et al. 2015).

Climate change related range shifts to deeper waters have also been documented for many species of benthic marine invertebrates (Hiddink et al. 2014). Numerous potential

climate refugia are identified in the Northern Domain, nearby and deeper than existing colonies. Our results suggest strong down-current connections between existing colonies and potential climate refugia along the Scotian Slope and off New England to Norfolk Canyon. These strong connections, in combination with strong local retention in the LCCA and The Gully (identified in Chapter 2), suggest that the Northern Domain could be self- sustaining in the face of climate change. In contrast, SEUS populations form weak (<1%) connections with potential climate refugia, and only to Bermuda and NE England seamounts. Most SEUS populations experience severe habitat decline and are removed early in our analyses. If these connections are realized before the source nodes are lost to habitat decline, the refugia at Bermuda and NE England Seamounts could act as important spatio-temporal stepping stones, connecting present day *L. pertusa* populations with future suitable habitats further north (Huang et al. 2020).

3.5.3 Limitations

Our methods for simulating habitat loss were based on the degree of predicted habitat suitability at each node for 2081-2100 and removing them sequentially from lowest HS to highest HS. The ranking of absolute HS scores likely does not translate directly to the temporal order in which populations of *L. pertusa* will become locally extinct with climate change. It is also possible that the HS values at which habitat becomes unsuitable differ among geographic areas and nodes are removed from the network in a different sequence than predicted in our analyses. However, we believe our analyses reveal likely changes and degradation to the overall connectivity network in the NW Atlantic, with

increasing decline in suitable habitat for *L. pertusa* irrespective of the order of node removal. Further, our chosen habitat suitability model does not account for changes in ocean currents with climate change, and velocity and temperature changes will likely have a non-zero impact on larval dispersal and the connections between nodes. We account for this in the identification of climate refugia by selecting areas which are also suitable during present-day conditions and can theoretically be colonized by larval dispersal through present-day oceanographic conditions; however, we have no way to account for changes in ocean currents during the habitat removal simulation.

3.5.4 Conclusions

We observed major impacts to the network as increasingly more suitable habitat of *L. pertusa* was removed due to climate change: first, a halt in bi-directional transport between south and north of Cape Hatteras and a potential strengthening of a biogeographic barrier, and secondly the separation of all three domain divisions. The Northern Domain is most likely to persist in the face of changing climate conditions, evidenced by the high number of potential climate refugia, strong connections from existing *L. pertusa* populations to these refugia, and high local retention rates in the LCCA and The Gully (Chapter 2). The GOM and SEUS are likely more vulnerable to extinction due to greater declines in suitable habitat, increased separation of nodes, less larval input, fewer potential climate refugia, and weaker connections to climate refugia. Our dispersal simulations indicate that the predicted northward expansion of suitable habitat may not be connected to *L. pertusa* populations due to the prevailing currents in

the region. This suggests that *L. pertusa*, as well as other deep-sea benthic invertebrates in the Northwest Atlantic, may have little ability to adapt to climate change by shifting their ranges northward. These results underscore the importance of considering dispersal pathways when evaluating potential range expansion for species with a prevalent larval stage. As our results show, a break down of connectivity between subpopulations may not put an entire metapopulation at risk of extinction, some portion or section may be able to persist, depending on the network characteristics. As climate change progresses and the dynamics of marine systems change, increased research focused on the direct impacts of climate change on larval dispersal, and thus connectivity, will be integral to understanding how and if species are able to adapt to these changing conditions.

Chapter 4

Discussion

Population connectivity is considered a governing process in the spatial distribution, health, and resilience of metapopulations and is integral to our understanding of how ecosystems function. Yet, connectivity is also one of the most difficult processes to quantify. The suite of environmental and species-specific biological traits that influence connectivity can be difficult to measure and parameterize, particularly for data-poor deep-sea species.

In this thesis, I address the uncertainties in larval life-history traits by parameterizing life-history trait ranges which overlap measured values from samples obtained in the Northeast Atlantic Ocean. In **Chapter 2**, I use biophysical modelling and graph theory to describe and characterize the spatial and temporal connectivity dynamics of an ecologically important deep-water coral, *Lophelia pertusa*. By exploring a range of biological parameters, I determine that the timing of spawning (which is currently unknown for *L. pertusa* in the NW Atlantic) does not affect the dominant patterns of potential connectivity, whereas larval development and swimming behaviour do significantly so. I document a two-fold increase in potential connectivity probability in larvae competent to settle at 20 days compared to 30 days, as well as larvae with an age-dependent swimming ability compared to a constant swimming velocity. The results of these analyses suggest that the lack of information available on biological traits for deep-sea species should not inhibit connectivity analyses; meaningful estimates of connectivity can still be achieved for deep-sea species without clearly resolved life-history traits. In

addition, due to the range of values for biological variables explored in our model, these results could be used to infer potential connectivity for other deep-sea species occupying similar habitat with comparable life history stages in the NW Atlantic Ocean.

For *L. pertusa* in the NW Atlantic, the strength of potential connections between populations are spatially distinct. In the Northern Domain (ranging from New England to Nova Scotia), strong potential connections exist from canyons off New England southwestwards toward Cape Hatteras. Populations surrounding Cape Hatteras are identified as the only subpopulations facilitating larval exchange between the Northern Domain and the Southeastern United States (ranging from southern Florida to Cape Hatteras). I document strong retention in the Gulf of Mexico, Norfolk Canyon, the *Lophelia* Coral Conservation Area and the Gully, suggesting these areas can persist without larval input from other populations.

In **Chapter 3**, I identify potential changes to the network because of habitat degradation caused by climate change. I find that the Gulf of Mexico and Southeastern United States are at risk of network breakdowns, whereas the Northern Domain is more likely to persist in a warming ocean. Bi-directional larval transport at Cape Hatteras halts at 20% habitat loss, and the SEUS and GOM became separated from each other at 60% habitat loss. I also find limited potential for *L. pertusa* to colonize climate refugia and predicted suitable habitats, likely due to the predominant equatorward flow of the Labrador Current. This research highlights that climate change related habitat loss can have drastic impacts on potential connectivity in subregions of a deep-sea metapopulation, while other regions of the metapopulation may be more likely to persist in a changing ocean.

Together, these studies focus on a deep-sea species with the potential for long distance larval dispersal, as well as localized high-probability connections between subpopulations, and region-specific potential to adapt to a changing ocean. This research contributes to the limited repository of deep-sea connectivity research and improves our understanding of population dynamics for an ecologically important species.

References:

Addamo AM, Vertino A, Stolarski J, García-Jiménez R, Taviani M, Machordom A (2016) Merging scleractinian genera: the overwhelming genetic similarity between solitary Desmophyllum and colonial Lophelia. BMC Evolutionary Biology 16:108. doi: 10.1186/s12862-016-0654-8

Artzy-Randrup Y, Stone L (2010) Connectivity, Cycles, and Persistence Thresholds in Metapopulation Networks. PLoS Comput Biol 6:e1000876. doi: 10.1371/journal.pcbi.1000876

Assis J, Failler P, Fragkopoulou E, Abecasis D, Touron-Gardic G, Regalla A, Sidina E, Dinis H, Serrao EA (2021) Potential Biodiversity Connectivity in the Network of Marine Protected Areas in Western Africa. Front Mar Sci 8:765053. doi: 10.3389/fmars.2021.765053

Auscavitch SR, Deere MC, Keller AG, Rotjan RD, Shank TM, Cordes EE (2020) Oceanographic Drivers of Deep-Sea Coral Species Distribution and Community Assembly on Seamounts, Islands, Atolls, and Reefs Within the Phoenix Islands Protected Area. Frontiers in Marine Science. doi: 10.3389/fmars.2020.00042

Baillon S, Hamel J-F, Wareham VE, Mercier A (2012) Deep cold-water corals as nurseries for fish larvae. Frontiers in Ecology and the Environment 10:351–356.

Baillon S, Hamel J-F, Wareham VE, Mercier A (2014) Seasonality in reproduction of the deep-water pennatulacean coral Anthoptilum grandiflorum. Mar Biol 161:29–43. doi: 10.1007/s00227-013-2311-8

Beaugrand G (2009) Decadal changes in climate and ecosystems in the North Atlantic Ocean and adjacent seas. Deep Sea Research Part II: Topical Studies in Oceanography 56:656–673. doi: 10.1016/j.dsr2.2008.12.022

Berumen ML, Almany GR, Planes S, Jones GP, Saenz-Agudelo P, Thorrold SR (2012) Persistence of self-recruitment and patterns of larval connectivity in a marine protected area network. Ecology and Evolution 2:444–452. doi: 10.1002/ece3.208

Bisagni JJ, Gangopadhyay A, Sanchez-Franks A (2017) Secular change and inter-annual variability of the Gulf Stream position, 1993–2013, 70°−55°W. Deep Sea Research Part I: Oceanographic Research Papers 125:1–10. doi: 10.1016/j.dsr.2017.04.001

Bode M, Burrage K, Possingham HP (2008) Using complex network metrics to predict the persistence of metapopulations with asymmetric connectivity patterns. Ecological Modelling 214:201–209. doi: 10.1016/j.ecolmodel.2008.02.040

Brito-Morales I, Schoeman DS, Molinos JG, Burrows MT, Klein CJ, Arafeh-Dalmau N, Kaschner K, Garilao C, Kesner-Reyes K, Richardson AJ (2020) Climate velocity reveals increasing exposure of deep-ocean biodiversity to future warming. Nature Climate Change 10:576–581. doi: 10.1038/s41558-020-0773-5

Brooke S, Ross SW (2014) First observations of the cold-water coral Lophelia pertusa in mid-Atlantic canyons of the USA. Deep Sea Research Part II: Topical Studies in Oceanography 104:245–251. doi: 10.1016/j.dsr2.2013.06.011

Brooke S, Schroeder WW (2007) State of Deep Coral Ecosystems in the Gulf of Mexico Region: Texas to the Florida Straits. 37.

Brooke S, Ross SW, Bane JM, Seim HE, Young CM (2013) Temperature tolerance of the deep-sea coral Lophelia pertusa from the southeastern United States. Deep Sea Research Part II: Topical Studies in Oceanography 92:240–248. doi: 10.1016/j.dsr2.2012.12.001

Bryan-Brown DN, Brown CJ, Hughes JM, Connolly RM (2017) Patterns and trends in marine population connectivity research. Marine Ecology Progress Series 585:243–256. doi: 10.3354/meps12418

Buhl-Mortensen P, Gordon DC, Buhl-Mortensen L, Kulka DW (2017) First description of a Lophelia pertusa reef complex in Atlantic Canada. Deep Sea Research Part I: Oceanographic Research Papers 126:21–30. doi: 10.1016/j.dsr.2017.05.009

Burgess SC, Nickols KJ, Griesemer CD, Barnett LAK, Dedrick AG, Satterthwaite EV, Yamane L, Morgan SG, White JW, Botsford LW (2014) Beyond connectivity: how empirical methods can quantify population persistence to improve marine protected-area design. Ecological Applications 24:257–270. doi: https://doi.org/10.1890/13-0710.1

Burrows M, Schoeman D, Buckley L, Moore P, Poloczanska E, Brander K, Brown C, Bruno J, Duarte C, Halpern B, Holding J, Kappel C, Kiessling W, O'Connor M, Pandolfi J, Parmesan C, Schwing F, Sydeman W, Richardson A (2011) The Pace of Shifting Climate in Marine and Terrestrial Ecosystems. Science (New York, NY) 334:652–5. doi: 10.1126/science.1210288

Cardona Y, Ruiz-Ramos DV, Baums IB, Bracco A (2016) Potential Connectivity of Coldwater Black Coral Communities in the Northern Gulf of Mexico. PLOS ONE 11:e0156257. doi: 10.1371/journal.pone.0156257

Cecino G, Treml EA (2021) Local connections and the larval competency strongly influence marine metapopulation persistence. Ecological Applications 31:e02302. doi: 10.1002/eap.2302

Connolly SR, Baird AH (2010) Estimating dispersal potential for marine larvae: dynamic models applied to scleractinian corals. Ecology 91:3572–3583. doi: 10.1890/10-0143.1

Cowen R, Gawarkiewicz G, Pineda J, Thorrold S, Werner F (2007) Population Connectivity in Marine Systems: An Overview. Oceanog 20:14–21. doi: 10.5670/oceanog.2007.26

Cowen RK, Sponaugle S (2009) Larval Dispersal and Marine Population Connectivity. Annu Rev Mar Sci 1:443–466. doi: https://doi.org/10.1146/annurev.marine.010908.163757

Cowen RK, Paris CB, Srinivasan A (2006) Scaling of Connectivity in Marine Populations. Science 311:522–527. doi: 10.1126/science.1122039

De Clippele LH, Buhl-Mortensen P, Buhl-Mortensen L (2015) Fauna associated with cold water gorgonians and sea pens. Continental Shelf Research 105:67–78. doi: https://doi.org/10.1016/j.csr.2015.06.007

DeHaan CJ, Sturges W (2005) Deep Cyclonic Circulation in the Gulf of Mexico. Journal of Physical Oceanography 35:1801–1812. doi: 10.1175/JPO2790.1

Delandmeter P, van Sebille E (2019) The Parcels v2.0 Lagrangian framework: new field interpolation schemes. Geoscientific Model Development 12:3571–3584. doi: 10.5194/gmd-12-3571-2019

Fox AD, Henry L-A, Corne DW, Roberts JM (2016) Sensitivity of marine protected area network connectivity to atmospheric variability. R Soc open sci 3:160494. doi: 10.1098/rsos.160494

Gary SF, Fox AD, Biastoch A, Roberts JM, Cunningham SA (2020) Larval behaviour, dispersal and population connectivity in the deep sea. Scientific Reports 10:10675. doi: 10.1038/s41598-020-67503-7

Gasbarro R, Sowers D, Margolin A, Cordes EE (2022) Distribution and predicted climatic refugia for a reef-building cold-water coral on the southeast US margin. Global Change Biology 28:7108–7125. doi: 10.1111/gcb.16415

Gunderson A, Stillman J (2015) Plasticity in thermal tolerance has limited potential to buffer ectotherms from global warming. Proceedings of the Royal Society B: Biological Sciences. doi: 10.1098/rspb.2015.0401

Han G, Ohashi K, Chen N, Myers PG, Nunes N, Fischer J (2010) Decline and partial rebound of the Labrador Current 1993-2004: Monitoring ocean currents from altimetric and conductivity-temperature-depth data. Journal of Geophysical Research Oceans. doi: 10.1029/2009JC006091

Handmann P, Fischer J, Visbeck M, Karstensen J, Biastoch A, Böning C, Patara L (2018) The Deep Western Boundary Current in the Labrador Sea From Observations and a High-Resolution Model. Journal of Geophysical Research: Oceans 123:2829–2850. doi: 10.1002/2017JC013702

Hanski I (1999) Habitat Connectivity, Habitat Continuity, and Metapopulations in Dynamic Landscapes. Oikos 87:209–219. doi: 10.2307/3546736

Harrison P (2011) Sexual reproduction of scleractinian corals - Southern Cross University. In: Coral reefs: an ecosystem in transition. pp 59–85

Hiddink J, Burrows M, Molinos J (2014) Temperature tracking by North Sea benthic invertebrates in response to climate change. Global Change Biology. doi: 10.1111/gcb.12726

Hilário A, Metaxas A, Gaudron SM, Howell KL, Mercier A, Mestre NC, Ross RE, Thurnherr AM, Young C (2015) Estimating dispersal distance in the deep sea: challenges and applications to marine reserves. Front Mar Sci. doi: 10.3389/fmars.2015.00006

Hogan JD, Thiessen RJ, Sale PF, Heath DD (2012) Local retention, dispersal and fluctuating connectivity among populations of a coral reef fish. Oecologia 168:61–71. doi: 10.1007/s00442-011-2058-1

Huang J-L, Andrello M, Martensen AC, Saura S, Liu D-F, He J-H, Fortin M-J (2020) Importance of spatio–temporal connectivity to maintain species experiencing range shifts. Ecography 43:591–603. doi: 10.1111/ecog.04716

Kang D, Curchitser EN, Rosati A (2016) Seasonal Variability of the Gulf Stream Kinetic Energy. Journal of Physical Oceanography 46:1189–1207. doi: 10.1175/JPO-D-15-0235.1

Kenchington E, Yashayaev I, Tendal OS, Jørgensbye H (2017) Water mass characteristics and associated fauna of a recently discovered Lophelia pertusa (Scleractinia: Anthozoa) reef in Greenlandic waters. Polar Biol 40:321–337. doi: 10.1007/s00300-016-1957-3

Krumhansl K, Gentleman W, Lee K, Ramey-Balci P, Goodwin J, Wang Z, Lowen B, Lyons D, Therriault TW, DiBacco C (2023) Permeability of coastal biogeographic barriers to marine larval dispersal on the east and west coasts of North America. Global Ecol Biogeogr 32:945–961. doi: 10.1111/geb.13654

Larsson AI, Järnegren J, Strömberg SM, Dahl MP, Lundälv T, Brooke S (2014) Embryogenesis and Larval Biology of the Cold-Water Coral Lophelia pertusa. PLOS ONE 9:e102222. doi: 10.1371/journal.pone.0102222

Leicht EA, Newman MEJ (2008) Community Structure in Directed Networks. Phys Rev Lett 100:118703. doi: 10.1103/PhysRevLett.100.118703

Lett C, Nguyen-Huu T, Cuif M, Saenz-Agudelo P, Kaplan DM (2015) Linking local retention, self-recruitment, and persistence in marine metapopulations. Ecology 96:2236–2244. doi: https://doi.org/10.1890/14-1305.1

Liu G, Bracco A, Quattrini AM, Herrera S (2021) Kilometer-Scale Larval Dispersal Processes Predict Metapopulation Connectivity Pathways for Paramuricea biscaya in the Northern Gulf of Mexico. Front Mar Sci 8:790927. doi: 10.3389/fmars.2021.790927

Lunden JJ, McNicholl CG, Sears CR, Morrison CL, Cordes EE (2014) Acute survivorship of the deep-sea coral Lophelia pertusa from the Gulf of Mexico under acidification, warming, and deoxygenation.

Matos FL, Aguzzi J, Company JB, Cunha MR (2023) Gone with the stream: Functional connectivity of a cold-water coral at basin scale. Limnology and Oceanography. doi: 10.1002/lno.12444

Meinshausen M, Lewis J, McGlade C, Gütschow J, Nicholls Z, Burdon R, Cozzi L, Hackmann B (2022) Realization of Paris Agreement pledges may limit warming just below 2 °C. Nature 604:304–309. doi: 10.1038/s41586-022-04553-z

Mercier A, Sun Z, Hamel J-F (2011) Reproductive periodicity, spawning and development of the deep-sea scleractinian coral Flabellum angulare. Mar Biol 158:371–380. doi: 10.1007/s00227-010-1565-7

Mienis F, Duineveld GCA, Davies AJ, Ross SW, Seim H, Bane J, van Weering TCE (2012) The influence of near-bed hydrodynamic conditions on cold-water corals in the Viosca Knoll area, Gulf of Mexico. Deep Sea Research Part I: Oceanographic Research Papers 60:32–45. doi: 10.1016/j.dsr.2011.10.007

Morato T, González-Irusta J-M, Dominguez-Carrió C, Wei C-L, Davies A, Sweetman AK, Taranto GH, Beazley L, García-Alegre A, Grehan A, Laffargue P, Murillo FJ, Sacau M, Vaz S, Kenchington E, Arnaud-Haond S, Callery O, Chimienti G, Cordes E, Egilsdottir H, Freiwald A, Gasbarro R, Gutiérrez-Zárate C, Gianni M, Gilkinson K, Hayes VEW, Hebbeln D, Hedges K, Henry L-A, Johnson D, Koen-Alonso M, Lirette C, Mastrototaro F, Menot L, Molodtsova T, Muñoz PD, Orejas C, Pennino MG, Puerta P, Ragnarsson SÁ, Ramiro-Sánchez B, Rice J, Rivera J, Roberts JM, Ross SW, Rueda JL, Sampaio Í, Snelgrove P, Stirling D, Treble MA, Urra J, Vad J, Oevelen D van, Watling L, Walkusz W, Wienberg C, Woillez M, Levin LA, Carreiro-Silva M (2020) Climate-induced changes in the suitable habitat of cold-water corals and commercially important deep-sea fishes in the North Atlantic. Global Change Biology 26:2181–2202. doi: https://doi.org/10.1111/gcb.14996

Morrison CL, Ross SW, Nizinski MS, Brooke S, Järnegren J, Waller RG, Johnson RL, King TL (2011) Genetic discontinuity among regional populations of Lophelia pertusa in the North Atlantic Ocean. Conserv Genet 12:713–729. doi: 10.1007/s10592-010-0178-5

O'Connor MI, Bruno JF, Gaines SD, Halpern BS, Lester SE, Kinlan BP, Weiss JM (2007) Temperature control of larval dispersal and the implications for marine ecology, evolution, and conservation. Proc Natl Acad Sci USA 104:1266–1271. doi: 10.1073/pnas.0603422104

Okubo A (1971) Oceanic diffusion diagrams. Deep Sea Research and Oceanographic Abstracts 18:789–802. doi: 10.1016/0011-7471(71)90046-5

Ospina-Alvarez A, de Juan S, Alós J, Basterretxea G, Alonso-Fernández A, Follana-Berná G, Palmer M, Catalán I (2020) MPA network design based on graph theory and emergent properties of larval dispersal. Mar Ecol Prog Ser 650:309–326. doi: https://doi.org/10.3354/meps13399

Pappalardo P, Pringle JM, Wares JP, Byers JE (2015) The location, strength, and mechanisms behind marine biogeographic boundaries of the east coast of North America. Ecography 38:722–731. doi: 10.1111/ecog.01135

Parmesan C, Gaines S, Gonzalez L, Kaufman DM, Kingsolver J, Townsend Peterson A, Sagarin R (2005) Empirical perspectives on species borders: from traditional biogeography to global change. Oikos 108:58–75. doi: 10.1111/j.0030-1299.2005.13150.x

Peterson I, Greenan B, Gilbert D, Hebert D (2017) Variability and wind forcing of ocean temperature and thermal fronts in the Slope Water region of the Northwest Atlantic. Journal of Geophysical Research: Oceans 122:7325–7343. doi: https://doi.org/10.1002/2017JC012788

Pineda J, HARE JA, SPONAUGLE S (2007) Larval Transport and Dispersal in the Coastal Ocean and Consequences for Population Connectivity. Oceanography 20:22–39.

Pinsky ML, Eikeset AM, McCauley DJ, Payne JL, Sunday JM (2019) Greater vulnerability to warming of marine versus terrestrial ectotherms. Nature 569:108–111. doi: 10.1038/s41586-019-1132-4

Pinsky ML, Selden RL, Kitchel ZJ (2020) Climate-Driven Shifts in Marine Species Ranges: Scaling from Organisms to Communities. Annu Rev Mar Sci 12:153–179. doi: 10.1146/annurev-marine-010419-010916

Pires DO, Silva JC, Bastos ND (2014) Reproduction of deep-sea reef-building corals from the southwestern Atlantic. Deep Sea Research Part II: Topical Studies in Oceanography 99:51–63. doi: 10.1016/j.dsr2.2013.07.008

Poloczanska E, Brown C, Sydeman W, Kiessling W, Schoeman D, Moore P, Brander K, Bruno J, Buckley L, Burrows M (2013) Global imprint of climate change on marine life. Nature Climate Change. doi: 10.1038/nclimate1958

Reed JK, Weaver DC, Pomponi SA (2006) Habitat and Fauna of Deep-Water Lophelia pertusa Coral Reefs off the Southeastern U.S.: Blake Plateau, Straits of Florida, and Gulf of Mexico.

Ross SW, Nizinski MS (2007) State of Deep Coral Ecosystems in the U.S. Southeast Region: Cape Hatteras to Southeastern Florida. 38.

Ross SW, Brooke S, Quattrini AM, Rhode M, Watterson JC (2015) A deep-sea community, including Lophelia pertusa, at unusually shallow depths in the western North Atlantic Ocean off northeastern Florida. Mar Biol 162:635–648. doi: 10.1007/s00227-015-2611-2

Rossby T, Benway RL (2000) Slow variations in mean path of the Gulf Stream east of Cape Hatteras. Geophysical Research Letters 27:117–120. doi: 10.1029/1999GL002356

Rossby T, Bower AS, Shaw P-T (1985) Particle Pathways in the Gulf Stream. Bull Amer Meteor Soc 66:1106–1110. doi: 10.1175/1520-0477(1985)066<1106:PPITGS>2.0.CO;2

Roughan M, Macdonald HS, Baird ME, Glasby TM (2011) Modelling coastal connectivity in a Western Boundary Current: Seasonal and inter-annual variability. Deep Sea Research Part II: Topical Studies in Oceanography 58:628–644. doi: 10.1016/j.dsr2.2010.06.004

Savidge DK, Bane JM (2001) Wind and Gulf Stream influences on along-shelf transport and off-shelf export at Cape Hatteras, North Carolina. J Geophys Res 106:11505–11527. doi: 10.1029/2000JC000574

Seidov D, Mishonov A, Reagan J, Parsons R (2019) Resilience of the Gulf Stream path on decadal and longer timescales. Sci Rep 9:11549. doi: 10.1038/s41598-019-48011-9

Simons RD, Siegel DA, Brown KS (2013) Model sensitivity and robustness in the estimation of larval transport: A study of particle tracking parameters. Journal of Marine Systems 11.

Stanley RRE, DiBacco C, Lowen B, Beiko RG, Jeffery NW, Wyngaarden MV, Bentzen P, Brickman D, Benestan L, Bernatchez L, Johnson C, Snelgrove PVR, Wang Z, Wringe BF, Bradbury IR (2018) A climate-associated multispecies cryptic cline in the northwest Atlantic. Science Advances 4:eaaq0929. doi: 10.1126/sciadv.aaq0929

Strömberg SM, Larsson AI (2017) Larval Behavior and Longevity in the Cold-Water Coral Lophelia pertusa Indicate Potential for Long Distance Dispersal. Front Mar Sci. doi: 10.3389/fmars.2017.00411

Sundahl H, Buhl-Mortensen P, Buhl-Mortensen L (2020) Distribution and Suitable Habitat of the Cold-Water Corals Lophelia pertusa, Paragorgia arborea, and Primnoa resedaeformis on the Norwegian Continental Shelf. Front Mar Sci 7:213. doi: 10.3389/fmars.2020.00213

Sunday JM, Bates AE, Dulvy NK (2012) Thermal tolerance and the global redistribution of animals. Nature Clim Change 2:686–690. doi: 10.1038/nclimate1539

Sweetman AK, Thurber AR, Smith CR, Levin LA, Mora C, Wei C-L, Gooday AJ, Jones DOB, Rex M, Yasuhara M, Ingels J, Ruhl HA, Frieder CA, Danovaro R, Würzberg L, Baco A, Grupe BM, Pasulka A, Meyer KS, Dunlop KM, Henry L-A, Roberts JM (2017) Major impacts of climate change on deep-sea benthic ecosystems. Elementa: Science of the Anthropocene. doi: 10.1525/elementa.203

Tong R, Davies AJ, Purser A, Liu X, Liu F (2022) Global distribution of the cold-water coral Lophelia pertusa. IOP Conf Ser: Earth Environ Sci 1004:012010. doi: 10.1088/1755-1315/1004/1/012010

Townsend DW, Thomas AC, Mayer LM, Thomas MA, Quinlan JA (2006) Oceanography of the Northwest Atlantic continental shelf (1,W). In: The Sea. Harvard University Press, Cambridge, pp 119–168

Traag VA, Waltman L, van Eck NJ (2019) From Louvain to Leiden: guaranteeing well-connected communities. Sci Rep 9:5233. doi: 10.1038/s41598-019-41695-z

Treml EA, Ford JR, Black KP, Swearer SE (2015) Identifying the key biophysical drivers, connectivity outcomes, and metapopulation consequences of larval dispersal in the sea. Movement Ecology 3:17. doi: 10.1186/s40462-015-0045-6

Waller RG, Tyler PA (2005) The reproductive biology of two deep-water, reef-building scleractinians from the NE Atlantic Ocean. Coral Reefs 24:514. doi: 10.1007/s00338-005-0501-7

Wang S, Wang Z, Lirette C, Davies A, Kenchington E (2019) Comparison of Physical Connectivity Particle Tracking Models in the Flemish Cap Region. 46.

Wang S, Kenchington E, Wang Z, Davies AJ (2021) Life in the Fast Lane: Modeling the Fate of Glass Sponge Larvae in the Gulf Stream. Front Mar Sci 8:701218. doi: 10.3389/fmars.2021.701218

Wang S, Murillo F, Kenchington E (2022a) Climate-Change Refugia for the Bubblegum Coral Paragorgia arborea in the Northwest Atlantic. Frontiers in Marine Science 9:863693. doi: 10.3389/fmars.2022.863693

Wang Z, Bedford Institute of Oceanography, Canada, Department of Fisheries and Oceans (2018) BNAM: an eddy-resolving North Atlantic Ocean model to support ocean monitoring.

Wang Z, Yang J, Johnson C, DeTracey B (2022b) Changes in Deep Ocean Contribute to a “See-Sawing” Gulf Stream Path. Geophysical Research Letters 49:e2022GL100937. doi: 10.1029/2022GL100937

Wheeler A, A B, Freiwald A, Haas H, Huvenne V, Kozachenko M, Olu K, Opderbecke J (2007) Morphology and Environment of Deep-water Coral Mounds on the NW European Margin. International Journal of Earth Sciences (1437-3254) (Springer), 2007-02 , Vol 96 , N 1 , P 37-56. doi: 10.1007/s00531-006-0130-6

Wiens JJ (2016) Climate-Related Local Extinctions Are Already Widespread among Plant and Animal Species. PLOS Biology 14:e2001104. doi: 10.1371/journal.pbio.2001104

Wisshak M, Freiwald A, Lundälv T, Gektidis M (2005) The physical niche of the bathyal Lophelia pertusa in a non-bathyal setting: environmental controls and palaeoecological implications. In: Freiwald A, Roberts JM (eds) Cold-Water Corals and Ecosystems. Springer, Berlin, Heidelberg, pp 979–1001

Zheng M-D, Cao L (2014) Simulation of global ocean acidification and chemical habitats of shallow- and cold-water coral reefs. Advances in Climate Change Research 5:189–196. doi: 10.1016/j.accre.2015.05.002

Appendix A: Chapter 2

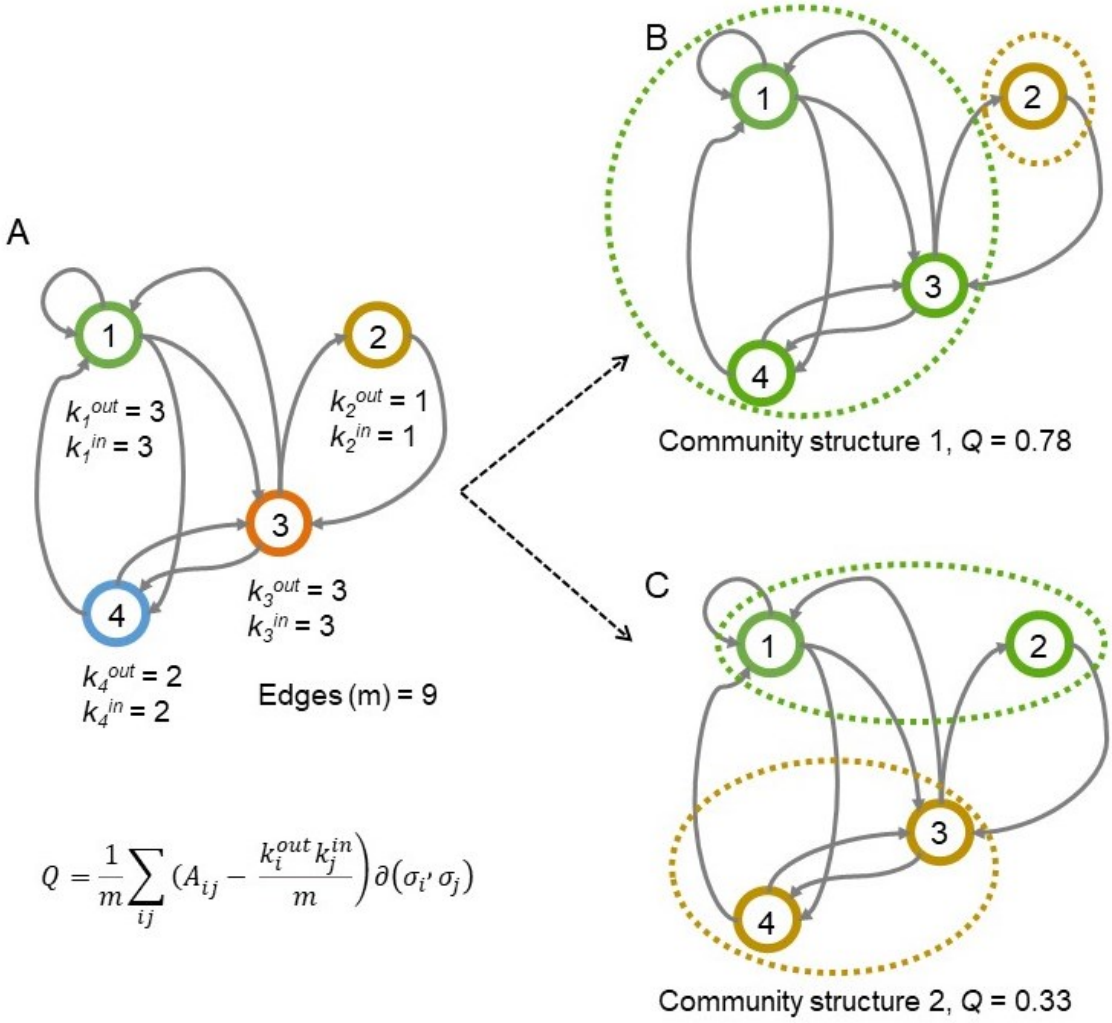

Figure A12 – Graphical representation of how the benefit function, Q, evaluates the strength of the community divisions within a network. **A**- A simple graph with 4 nodes and 9 total edges. **B**/**C**- Two possible decompositions of the graph into communities, with associated values of the benefit function. Between examples **B** and **C**, example **B** is the the strongest mathematical decomposition of the graph in **A**.

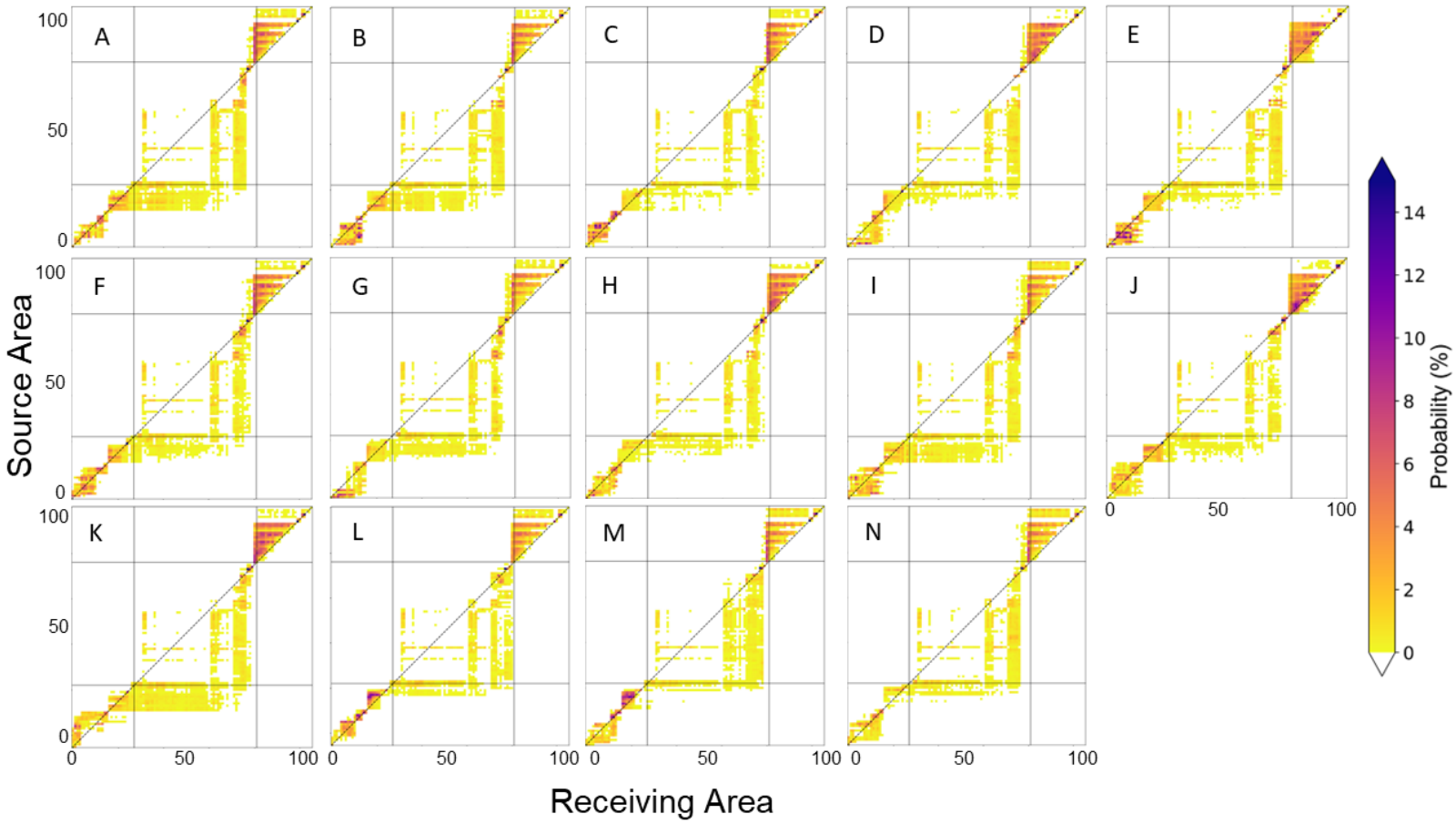

Figure A2– Connectivity matrices for each Winter from 2005 (**A**) – 2018 (**N**) for a 30-day pre-competency period and larval behaviour 1.

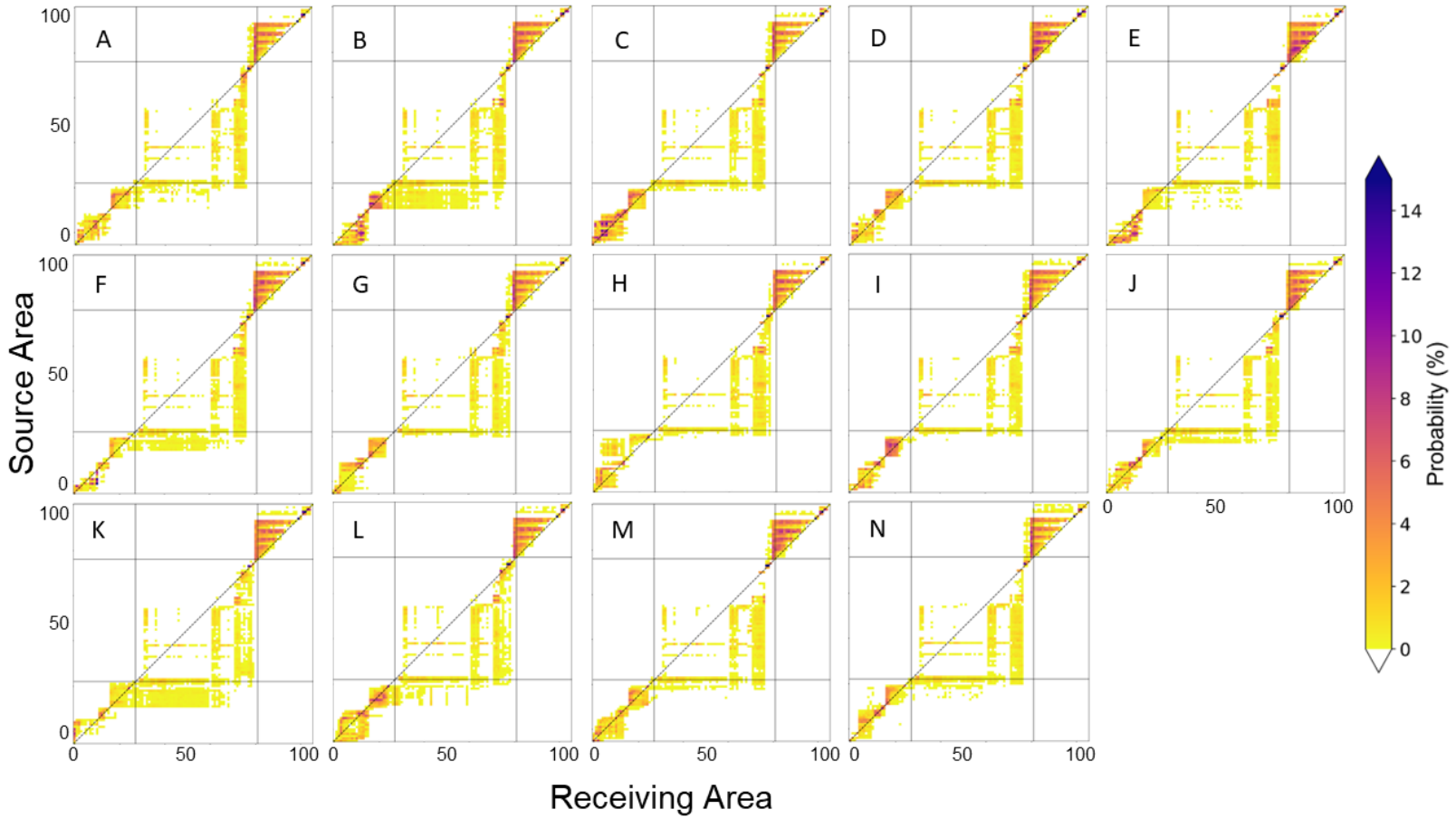

Figure A3 – Connectivity matrices for each Spring from 2005 (**A**) – 2018 (**N**) for a 30-day pre-competency period and larval behaviour 1.

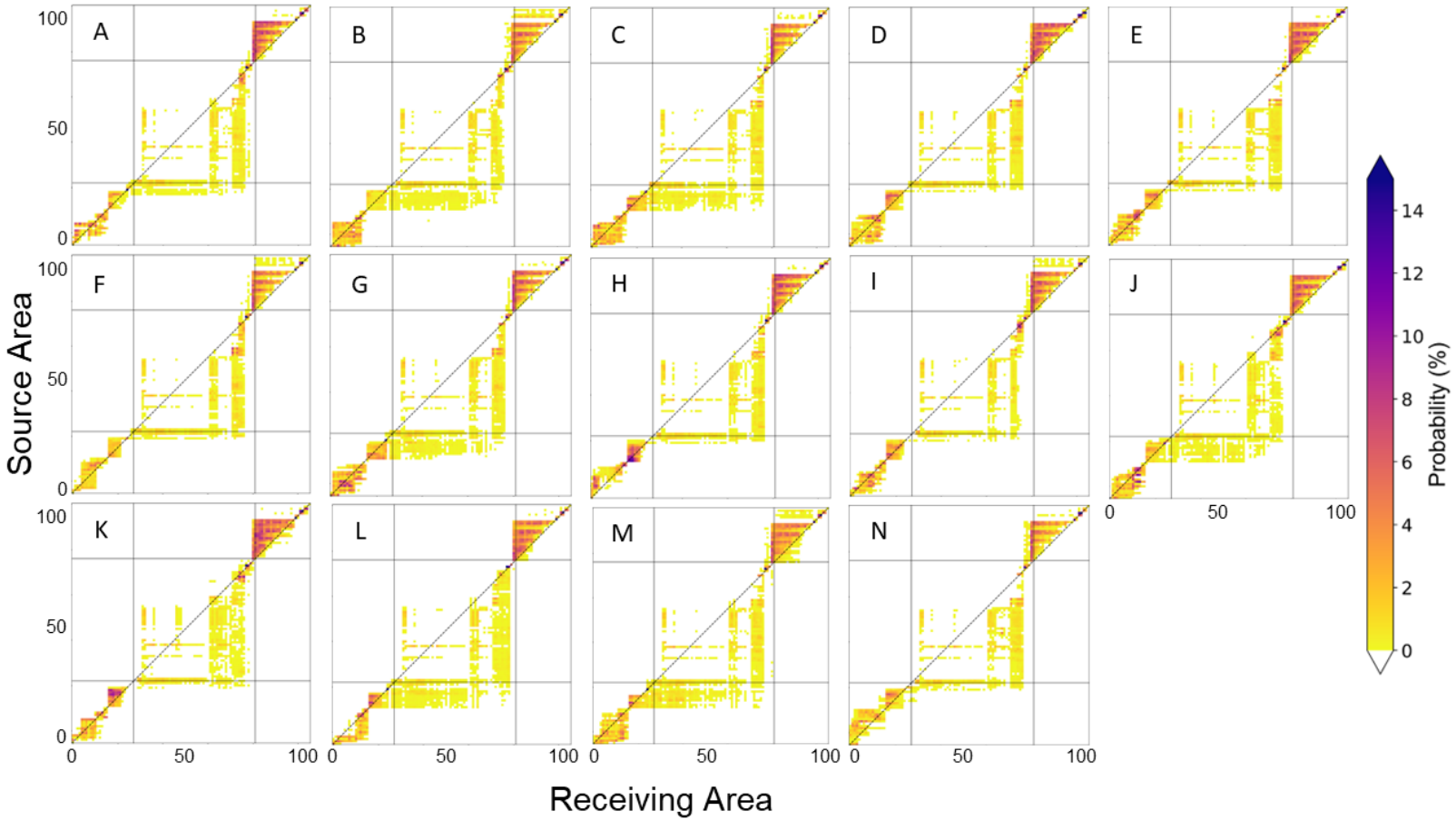

Figure A4 – Connectivity matrices for each Summer from 2005 (**A**) – 2018 (**N**) for a 30-day pre-competency period and larval behaviour 1.

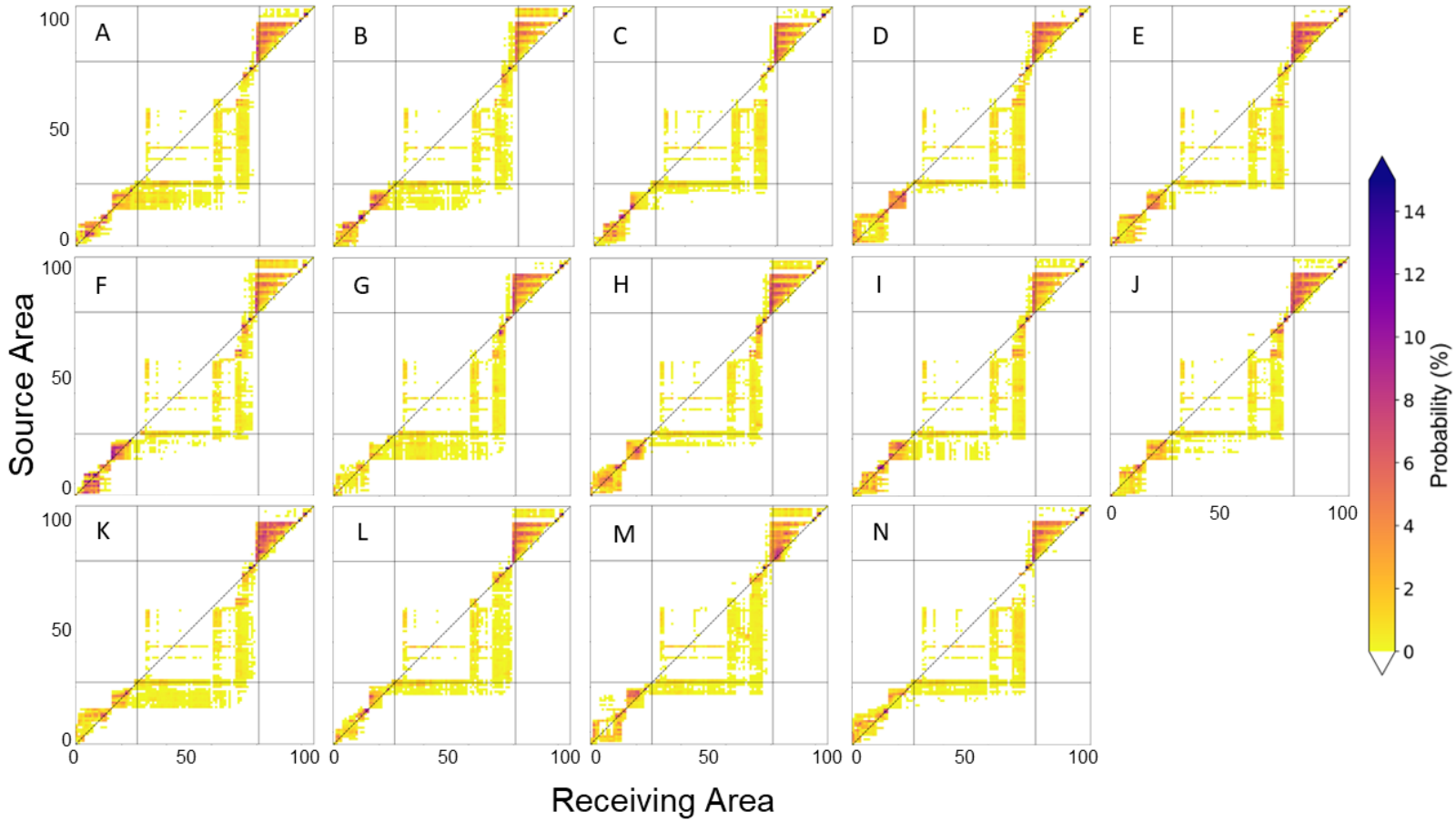

Figure A5 – Connectivity matrices for each Autumn from 2005 (**A**) – 2018 (**N**) for a 30-day pre-competency period and larval behaviour 1.

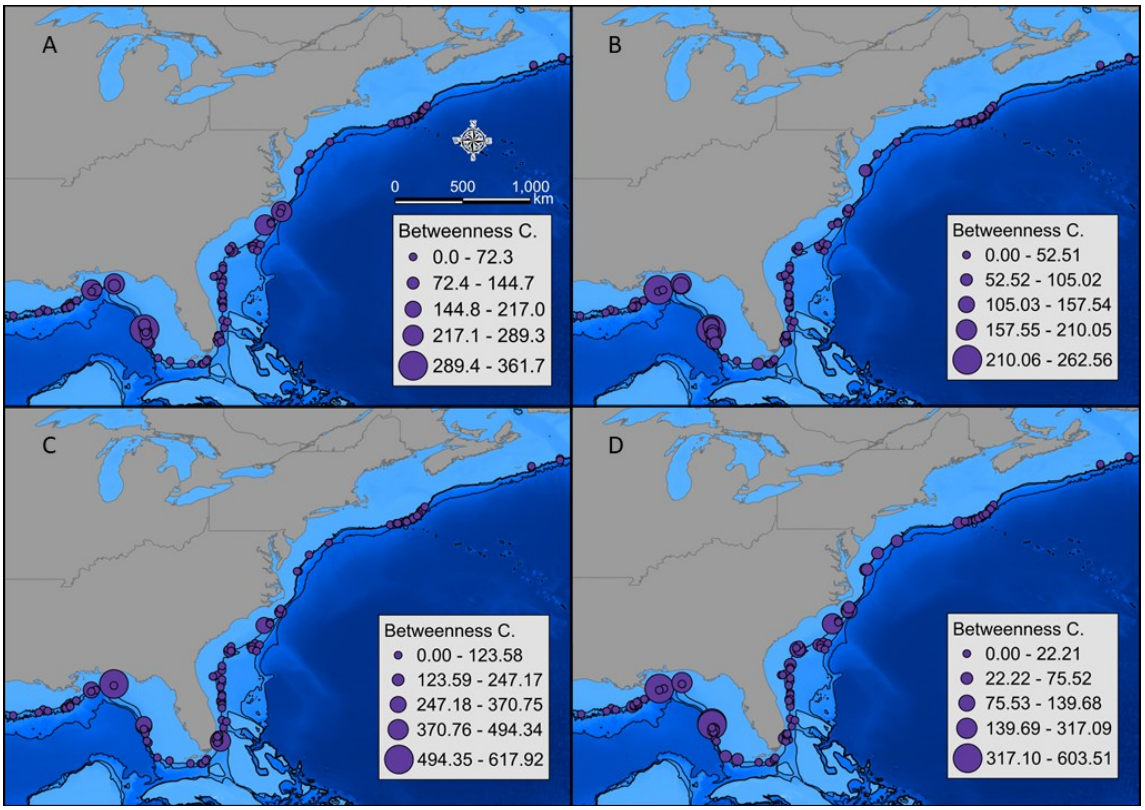

Figure A6 – Betweenness centrality scores for Winter (**A**), Spring (**B**), Summer (**C**) and Autumn (**D**), averaged over 2005-2018 for a 30-day pre-competency period and larval behaviour 1.

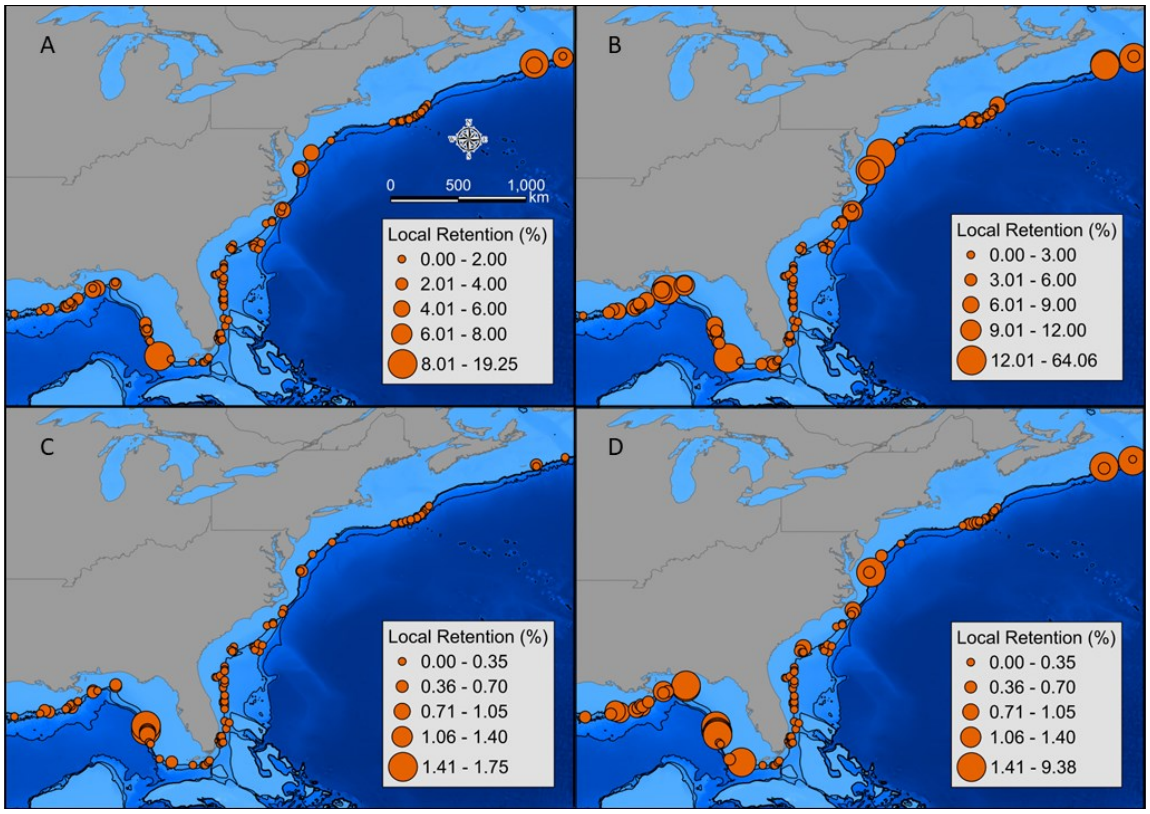

Figure A7 - Local retention for summer 2005-2018 for larval behaviour 1 and 30-day pre-competency period (**A**), larval behaviour 1 and 20-day pre-competency period (**B**), larval behaviour 2 and 30-day pre-competency period (**C**) and larval behaviour 2 and 20-day pre-competency period (**D**).

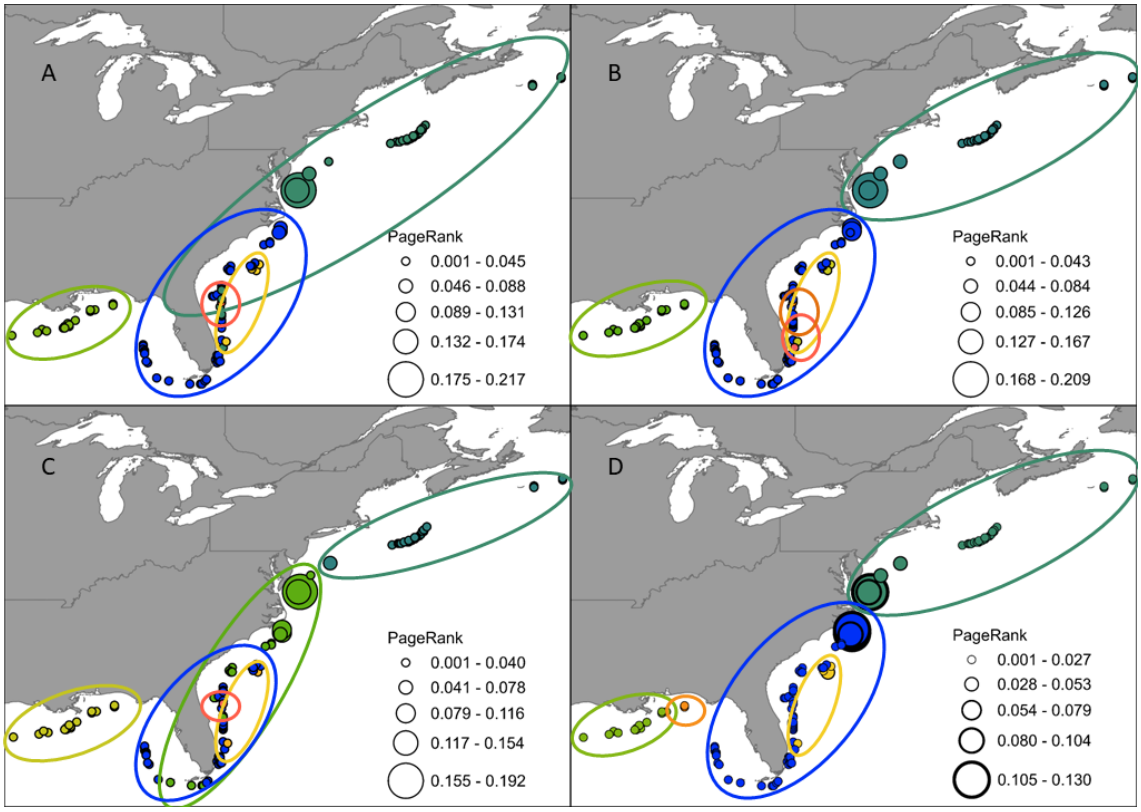

Figure A8 – Cluster groupings, identified by the colours of the nodes, and Google PageRank scores, represented by size of the nodes for Winter (**A**), Spring (**B**), Summer (**C**) and Autumn (**D**) averaged over 2005-2018 for larval behaviour 2 and 30-day pre-competency period.

Table A1– Data sources for Lophelia pertusa occurrence records used in analysis. Acronyms used are NOAA (National Oceanic and Atmospheric Administration), ROV (Remotely Operated Vehicle), HUD (Henry Hudson), LCCA (Lophelia Coral Conservation Area), MPA (Marine Protected Area), ROPOS (Remotely Operated Platform for Ocean Science), ECS (Eastern Canyons and Slope), HB (Henry Bigelow), USGS (United States Geological Survey), NMSH (National Museum of Natural History), HBOI (Harbour Branch Oceanographic Institute), BOEM (Bureau of Ocean Energy Management), PSU (Pennsylvania State University), NSUOC (Nova Southeastern University Oceanographic Center).

Research Survey ID/ Data Provider	Collection method	Date	Location
NOAA Okeanos Explorer EX1905	ROV survey	2019	Corsair Canyon
HUD2003059	Campod	2003	LCCA
HUD2009030	Campod	2009	LCCA
HUD2015011	4k Cam	2015	LCCA
HUD2001055	Campod	2001	The Gully MPA
HUD2007025	ROPOS	2007	ECS/ The Gully MPA
HUD2018021	Campod	2018	ECS/Rise/Abyss
HB1204TC05	Still image	2012-07-09	Middle Toms Canyon
HB1204TC16	Still image	2012-07-16	Gilbert Canyon
HB1302TC007	Still image	2013-06-15	Powell Canyon
HB1302TC008	Still image	2013-06-16	Powell Canyon
HB1302TC014	Still image	2013-06-19	Munson Canyon
HB1302TC017	Still image	2013-06-21	Munson Canyon
HB1302TC019	Still image	2013-06-22	Munson Canyon
HB1302TC021	Still image	2013-06-23	Munson Canyon
HB1504TC04	Still image	2015-07-29	Chebacco Canyon
HB1504TC04-2	Still image	2015-07-30	Chebacco Canyon
HB1504TC07	Still image	2015-08-02	Filebottom Canyon
HB1504TC14	Still image	2015-08-03	Welker Canyon
R1696	Still image	2014-06-20	Nygren Canyon
R1697	Still image	2014-06-21	Nygren-Heezen Intercanyon
R1698	Still image	2014-06-22	Heezen Canyon
R1699	Still image	2014-06-22	Heezen Canyon
R1701	Still image	2014-06-24	Corsair Canyon
R2006	Still image	2017-06-10	Munson-Nygren Intercanyon
R2007	Still image	2017-06-11	Munson-Nygren Intercanyon
R2008	Still image	2017-06-12	Kinlan
USGS	Submersible	1984-02-20	Little Bahama Bank

Table A1 continued…

Research Survey ID/ Data Provider	Collection method	Date	Location
USGS		1985	W Florida slope
NMSH		1983-11-12	Gulf of Mexico
Hall-Spencer et al. (2007)	ROV	2003-09-23	Gulf of Mexico
Hall-Spencer et al. (2007)		1984-11-12	Gulf of Mexico
NMSH	Submersible	1977-05-29	Little Bahama Bank
NMSH	Submersible	1984-02-21	West Of Little Bahama Bank
NMSH	Submersible	2004-07-25	Mississippi Canyon
NMSH	Submersible	2005-11-08	Cape Canaveral
NMSH	Submersible	1982-09-18	Lydonia Canyon
NMSH	ROV	2008-10-09	VK826/VK906
NMSH	Submersible	2004-06-15	Cape Lookout
NMSH	Submersible	2002-08-12	Cape Lookout
NMSH	Submersible	2005-09-20	Lophelia I | Lease Block VK826
Schmidt Ocean Institute	ROV	2012-08-31	Okeanos Ridge
Schmidt Ocean Institute	ROV	2012-12-09	Okeanos Ridge Deep Wall
HBOI	Submersible	2010-07-19	West Florida Lithoherm
BOEM	ROV	2009-08-20	West Florida Slope
NOAA	ROV	2012-03-20	Gulf of Mexico
NOAA	ROV	2014-04-28	Gulf of Mexico
NOAA	Submersible	2009-08-06	Triceratops
BOEM	Submersible	2005-09-08	Green Canyon 234
NOAA	ROV	2010-11-10	West Florida Slope
Temple University	ROV	2011-10-20	Viosca Knoll
Temple University	ROV	2010-07-25	Viosca Knoll
Temple University	ROV	2010-10-20	Louisiana Shelf
Temple University	ROV	2008-10-07	Viosca Knoll
Temple University	ROV	2009-09-03	Viosca Knoll
Temple University	AUV	2009-06-29	Viosca Knoll
Temple University	ROV	2008-09-26	Louisiana Shelf
HBOI	ROV	2011-09-25	Florida
HBOI	ROV	2011-06-03	Florida
NOAA	ROV	2010-04-12	Charleston Bump
USGS	ROV	2010-09-23	Viosca Knoll
USGS	Submersible	2009-09-16	West Florida Shelf

Table A1 continued…

Research Survey ID/ Data Provider	Collection method	Date	Location
BOEM	ROV	2013-05-06	Norfolk Canyon
BOEM	ROV	2012-09-12	Baltimore Canyon
NOAA	ROV	2017-08-14	Long Mound South
HBOI	Submersible	2002-08-19	South Carolina
HBOI	ROV	2003-09-12	Gulf Of Mexico
HBOI	Submersible	2004-05-21	Florida
HBOI	Submersible	2005-11-08	Florida
HBOI	Submersible	2006-06-02	Florida
PSU	ROV	2016-10-05	GC234
PSU	ROV	2015-05-02	MC751
NOAA	ROV	2017-11-30	South Reed
NOAA	ROV	2018-04-28	South of Long Mound
NOAA	ROV	2018-06-19	Blake Plateau
HBOI	ROV	2012-07-13	North Carolina
HBOI	ROV	2016-06-15	North Carolina
NSUOC	ROV	2011-01-26	Florida
NSUOC	ROV	2011-03-31	Florida